Around a mathematical model of the concomitant tumor resistance phenomenon

Laura Lumale, Sébastien Benzekry

Internship report
5GMM-MMN

Around a mathematical model of the concomitant tumor resistance phenomenon

Laura LUMALE

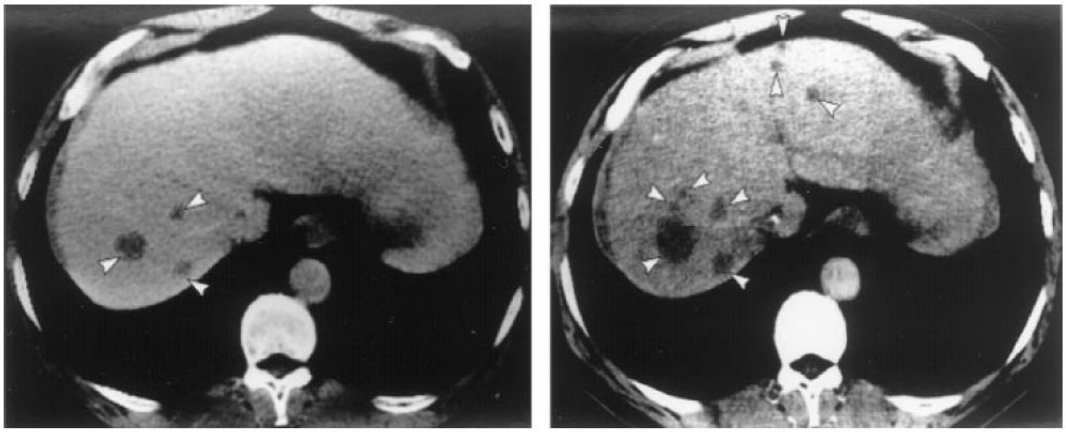

image credit: [Iwata et al., 2000], J Theor Biol, 2000

Supervised by : Sébastien Benzekry
October 30, 2016

INRIA-MONC
INSA de Toulouse

Internship report
5GMM-MMN

Around a mathematical model of the concomitant tumor resistance phenomenon

Laura LUMALE

Supervised by : Sébastien Benzekry
October 30, 2016

INRIA-MONC
INSA de Toulouse

Abstract

The phenomenon of concomitant resistance, discovered since 1906, traduces the inhibitory effect from a first tumor on the growth of a distant tumor. The importance of the investigation on the concomitant resistance was found following the removal of the primary tumor which could lead to dramatic clinical consequences due to the suppression of this inhibition : the post-surgery metastatic acceleration. We report here on a study of a mathematical model representing the concomitant resistance between two tumors in the same organism.
First, the study involves a statistical analysis of the tumor growth in 10 mice with a population approach:the non-linear mixed effect model which is the most common tool to describe the global behavior of all individuals. The goal was to compare different software which implement the method, where the function *NLME* on R has the fastest execution time.
Second, the study allows the validation of the concomitant resistance mathematical model on independent data thanks to the obtaining of a highest goodness-of-fit and a good prediction.
This study not only informs on the validity of the model but also provides a non-monotony of the metastatic acceleration depending on the volume of the tumor at the day of excision.

Acknowledgments

First, I would like to sincerely thank my tutor M. Benzekry for allowing me to do this enriching internship and to collaborate with his works, for welcoming me and integrating me in the team and for always being available.
Indeed, he gave me his passion for his work with enthusiasm and I discovered the usefulness of mathematics, an abstract discipline, with concrete applications in the biomedical field. He kept encouraging me and helping me throughout the internship.

I would also like to express my acknowledgments to all the team MONC who integrated me with solicitude and friendliness in a convivial and welcoming atmosphere. I think this kind of hospitality is very appreciated and also quite rare.

Thank you all

Contents

Introduction

During the 4th year as student at INSA Toulouse (Institut National des Sciences Appliquées), I had the opportunity to do an internship as part of one's school course at Inria (Institut national de recherche en informatique et en automatique) in Bordeaux which is a public research institution focusing on computer science and applied mathematics.
I worked for three months in MONC, a research team of Inria specialized in applications of mathematical modeling and simulations in Oncology.
Then, the context of my internship was the applied mathematics in the cancer research, a current issue, which was very enriching and complete because it gathered several fields and skills : the study of a mathematical model based on ordinary differential equations, the use of statistical tools and the assimilation of knowledge in cancer's biology.

Particularly, I was focusing on a cancer's curious phenomenon called «concomitant resistance»which was studied in pre-clinical experiments [Chiarella et al., 2012].
The concomitant resistant consists in the inhibition of a second tumor by the presence of a first tumor. Indeed, it involves that a primary tumor inhibits the growth of distant tumors (i.e metastasis) and also may lead them in dormancy.
The importance of this phenomenon occurs in some clinical results where the surgical removal of the tumor is followed by a dramatic acceleration of metastasis' growth due to the release of the inhibition exerted by the primary tumor which can lead to the death.

Thus, the goal of my internship was to get acquainted with articles from the literature about the phenomenon of concomitant resistance and with modeling works already made.
The aim was also to go into the study and the validation in depth of a mathematical model, formalized by M. Benzekry, representing this phenomenon and established from experiments involving the growth of two tumors in the same organism [Benzekry et al., 2016].

1 MONC of Inria a laboratory on applications of mathematical modeling in Oncology

1.1 Inria a public science and technology research institute

The Institut National de Recherche en Informatique et en Automatique (Inria) is a french national public research institution placed under the supervision of the French ministries of research and industry. It was created in 1967 and has 8 research centers in France whose CEO is Antoine Petit with a total budget of 230 million euros.
Inria is composed of 2700 employees from 87 different countries whose goal is to rise to the challenges of digital sciences which are involved in the future of our societies, regrouping the skills and talents of french and international researchers in computer sciences and applied mathematics.
Inria is tackling research subjects crucial to the current social issues and presents 4600 scientific publications per year in its scientific activities.

The original research model of Inria is that the research is organized in 178 «project teams »composed around 20 scientists (researchers, PhD students, engineers) sharing a common research program on a specific scientific topic.The project team is headed by a project team manager.
The advantage of project teams is that the team has a large measure of scientific and financial independence. Moreover, the teams may be associated with partner institutions (universities, schools, research organizations).
However, the Inria project-team has 4 years to achieve its objectives but it can be extended until a maximum lifetime of 12 years.
The general fields of scientific research at Inria are :

- Applied Mathematics, Computation and Simulation
- Algorithmic, Programming, Software and Architecture
- Networks, Systems and Services, Distributed Computing
- Perception, Cognition and Interaction
- Digital Health, Biology and Earth

Inria is able to provide an efficient response to the multidisciplinary challenges. Indeed, it transfers research results to companies (startups, SMEs and major groups) in various areas as health care, energy, security, transport, communication.

1.2 MONC an Inria project team on mathematical modeling in Oncology

Actually, the mathematics can apply to the health in many ways such as treat data from medical imaging to let doctors interpret it, prescribe quantities of treatment where the doses are adapted for the patient.
The use of digital sciences constantly progresses with the evolution of medical imaging and medical treatment, and is the current trend to be involved to do personalized medicine (as specify a treatment to a patient) or predictive medicine (as predict the effect and the efficient of a treatment).

Then, MONC is an Inria project team common with the University of Bordeaux, INP and CNRS, composed of 20 scientists (researchers, engineers, PhD students and even doctors) whose team leader is Olivier Saut.
The team works on problems of modeling in oncology. It is devoted to applications of mathematical modeling, simulations and scientific calculus in oncology to exploit available data.
The main goals of MONC are to develop personalized mathematical models for individualization of prognosis and treatments, to help the development of new therapies as electroporation or interventional radiology, and to ameliorate the understanding of cancer growth and metastasis by the construction of mathematical models able to reproduce and to predict the cancer's behavior.

The originality of this team is the collaboration between the mathematical researchers and the doctors specializing in oncology from CHU Bordeaux and the Institut Bergonie or with biologists from Bordeaux and Toulouse. The advantage is that this collaboration allows to help the interpretation of experiment results, to ameliorate the understanding of results and to extract the most information possible. Moreover, they can directly applied mathematical models of cancer's study on clinical data from imaging data (such as computed tomography images) of patients.

Recently, at the end of MONC research team's works, it has been created a startup named Nenuphar. It consists in the setting up of a software positioning and available for doctors. Nenuphar is capable of describe and model the lung metastasis' growth or the response to treatment.

2 Comparison of different tools implementing the NLME model for the analysis of the tumor's growth

For a first approach to the works effected by the team MONC about the tumors' behavior, I look into a statistic tool : the non linear mixed-effects (NLME) model which allows me to analyze data from a tumor's growth [Benzekry et al., 2014b] to a population scale.

The non linear mixed-effects model is an extension of the method of non-linear regression. We can extend to a population the results of a few individuals.
Mixed-effects modeling is the most used method for analysis of population approach, it can pool all the individual together and estimate a global distribution of the model parameters in the population.

The aim of our present is to compare the speed, efficiency and precision of several tools which implement this method for an unique model.

2.1 The Nonlinear Mixed-effects model for the population approach

2.1.1 Recall on the Linear Models

The matrix writing of the linear model is :

$$y = X\beta + \epsilon$$

where $y = (y_1, ..., y_i, ...y_n)'$ the vector $(n \times 1)$ of the n observations.
$X = \begin{pmatrix} X_{11} & ... & X_{1p} \\ ... & ... & ... \\ X_{i1} & ... & X_{ip} \\ ... & ... & ... \\ X_{n1} & ... & X_{np} \end{pmatrix}$ the matrix of the size $(n \times p)$
$\beta = (\beta_1, ...\beta_p)'$ the vector $(p \times 1)$ of the p parameters to estimate.
$\epsilon = (\epsilon_1, ..., \epsilon_n)'$ the vector $(n \times 1)$ of the residual errors where $\varepsilon_i \sim \mathcal{N}(0, \sigma^2)$.

To determine the estimate of the parameters β, we solve the problem of least square minimization on the function f defines like :

$$f(\beta) = \sum_{i=1}^{n} (Y_i - (X\beta)_i)^2 = ||Y - X\beta||^2 =< Y - X\beta, Y - X\beta >$$

We are looking $\hat{\beta}$ which minimizes $f(\beta)$ (i.e $\nabla f(\hat{\beta}) = 0$).

$$\nabla f(\beta + h) =< Y - X(\beta + h), Y - X(\beta + h) >$$

$$=< Y - X(\beta), Y - X(\beta) > +2 < Y - X\beta, Xh > +o(||h||)$$
$$= f(\beta) + \nabla f(\beta).h + o(||h||)$$

where $\nabla f(\beta) = 2X'(Y - X\beta)$.

Then, the solution of minimization is :

$$\nabla f(\beta) = 0 \leftrightarrow \hat{\beta} = \begin{pmatrix} \hat{\beta}_1 \\ \hat{\beta}_2 \\ ... \\ \hat{\beta}_p \end{pmatrix} = (X'X)^{-1}(X'Y)$$

2.1.2 Recall on the nonlinear Models

We can extend the linear model to more general ones where the observed phenomenon can be described mathematically (by structural model like differential equations). These nonlinear model have the form :

$$y_j = M(t_j, \Phi) + \varepsilon_j$$

for $j \in 1, ..., n$ individuals. where Φ is a vector of parameters for a structural model M. The model M is a nonlinear function of the components Φ.

2.1.3 The Nonlinear mixed-effects models

The main goal of the nonlinear mixed-effects models is to regroup all data together of all individuals and to extract a typical curve for the population.

A nonlinear mixed-effects model is described by :

$$y_{ij} = M(t_{ij}, \beta_i) + \epsilon_{ij}$$

with $\beta_i = \beta + \eta_i \sim N(\beta, \omega^2)$ and $\eta_i \sim N(0, \omega^2)$.

Where,

- y_{ij} is the j^{th} observation of the i individual at time t_{ij}.
- M is a nonlinear function of the components β_i composed of β and η_i.
- $\epsilon_i \sim N(0, \sigma^2)$ represent the residual errors.

– β represents the population parameter, also called *fixed effects*. We can note that they are often estimated by likelihood maximization performed, for instance, with the Stochastic Approximation of Expectation Maximization (SAEM) algorithm. It gives a general description of the observations of all individuals.

– $\eta_i \sim N(0, \omega^2)$ are the individual parameters, called *random effects*. They are distributed random variables in the population and allow to adapt the variability between individuals in the model.

2.2 The tools and software for the nonlinear mixed-effects models

- **Monolix :**
  Monolix is a non-free software specialized for nonlinear mixed-effects modeling (NLME) for pharmacometrics. It is based on the stochastic approximation expectation maximization (SAEM) algorithm computing the maximum likelihood estimator of the population parameters. It purposes an ergonomic interface which is easy to use with less programming. Monolix automatically generates a full set of diagnostic plots for example the Visual Predictive Check, Boxplot of the distribution of the effects random, Observation vs Prediction plot, Random effects,...
  To implement our Gompertz Model which is a ordinary differential equation, Monolix purpose to construct our model using Mlxtran. The model file contains the structural models.

- **NLME on R :**
  R is a programming language and software environment for statistical computing. It allows us to do a nonlinear mixed- effects model thanks to this package "NLME" which has a lot of functions whose *nlme* function. This function fits a nonlinear mixed-effects model :

  ```
  nlme(model, data, fixed, random, groups, start, correlation,
  weights, subset, method, na.action, naPattern, control, verbose)
  ```

  With NLME, the diagnostic plots are narrower than those Monolix.

- **SAEMIX on R :**
  SAEMIX is an R implementation of the Stochastic Approximation Expectation Minimization algorithm for parameter estimation in nonlinear mixed-effects models. It also computes the maximum likelihood estimator of the population parameters and provides standard errors for the maximum likelihood estimator. The

difficult with SAEMIX is that we need to adapt the writting of the data and the model according to SaemixData and SaemixModel. We can not just call the Gompertz function, we have to transform it in a saemixModel specifying the distribution for each parameter, the fixed estimate, the covariate model, ...
The SAEMIX package have as much diagnostic plots as Monolix.

- **NLMEFIT on Matlab :**
  Matlab is a numerical computing environment and programming langage which allows matrix manipulations, plotting of functions and data, implementation of algorithms.
  For the nonlinear mixed-effects, we use the *nlmefit* function in MATLAB which fits a nonlinear mixed-effects regression model and returns estimates of the fixed effects parameters.

2.3 The study of the tumor growth in 10 mice

To compare the performance of these different tools, we selected a common study which involves volume data of tumor growth for 10 mouses measured over several days [Benzekry et al., 2014b].
To understand the tumor's growth, in his article, [Benzekry et al., 2014b] compared the efficient of several mathematical models which attempt to describe and predict these experiments.

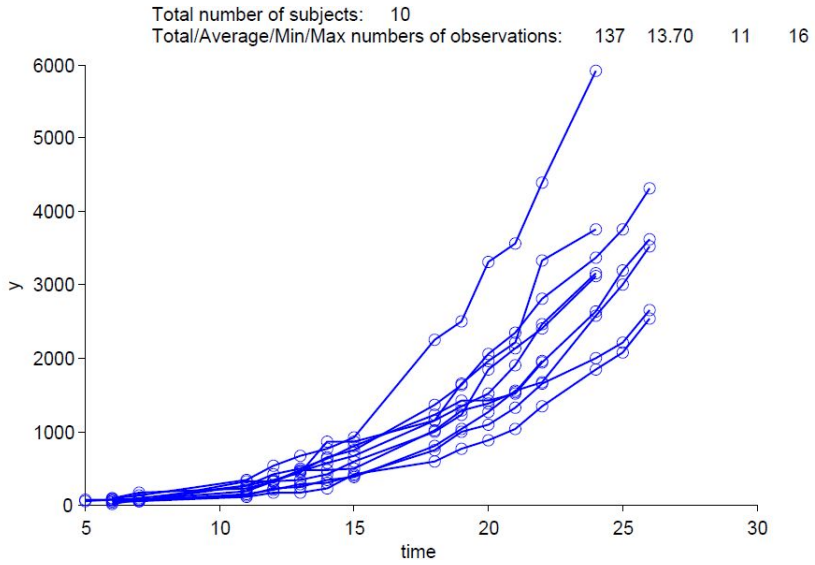

Figure 1: Volume of tumor data for 10 mices with Monolix

We take the Gompertz mathematical model for the tumor growth which reveals a very goodness-of-fit and allows to trace for each mice an individual fit. The Gompertz model is defined by :

$$\begin{cases} \frac{dV}{dt} = & ae^{-\beta t}V \\ V(t=0) = & 1\text{mm}^3 \end{cases} \tag{1}$$

whose the solution is :

$$V(t) = V_0 e^{\frac{a}{\beta}(1-e^{-\beta t})}$$

where V is the volume of tumor, a is the initial proliferation rate and β the rate of exponent decay of this proliferation rate.

Around the Gompertz model : This writing is non-autonomous and it can also be expressed by :

$$\begin{cases} \frac{dV}{dt} = & aVln(\frac{K}{V}) \\ V(t=0) = & 1\text{mm}^3 \end{cases}$$

This ordinary differential equation verifies the Cauchy problem where the solution exists and is unique :

$$V(t) = K^{(1-e^{-at})}$$

where K is the tumor size at the saturated level.

We can raise the question if the initial condition was $V(0) = 0$, a possible solution might be $V(t) = 0$.
Indeed, $f(V) = Vln(\frac{K}{V})$ is not lipschitz in 0 so it can not verify the Cauchy problem.
However, if we simplify the problem with $K = 1$,

$$\frac{dV}{dt} = -VlnV \Leftrightarrow \int_0^{V_1} \frac{dV}{-VlnV} = \int_0^{t_1} dt = t_1$$

It has no solution because according to Riemann theorem, the term on the left diverges and t_1 is a finite time.
Then, $V(t) = 0$ is the unique solution and the Gompertz model is well-posed in 0. It means that if the initial size of the tumor is 0 ($V(0) = 0$), we will not have any tumor ($V(t) = 0$) which is biologically acceptable.

Nevertheless, the problem is not well-posed for initial quantities of volume infinitely small ($V(0) \to 0$).

$$\frac{dV}{dt} = -VlnV = Vg(V)$$

with $g(V) = -lnV \underset{V\to 0}{\longrightarrow} +\infty$.
$g(V)$ represents the proliferation rate and this result means that the smaller the initial

volume of the tumor is, the more quickly it will grow which is biologically false. Indeed, a small tumor will take time to grow due to the cell division.

2.4 Analysis of results obtained for each method used

2.4.1 Comparison of the estimated parameters

Globally, all the tools used for the nonlinear mixed-effects model give us approximately the same values for the fixed effects and their standard errors. Nevertheless, according the method involved, we can reach more information about the model.
We summarize in a table the results with the time of execution for each method to better compare.
$a = 1$ and $\beta = 0.1$ are the initial values of the fixed effects.

		MONOLIX	NLME	SAEMIX	NLMEFIT
Fixed Effect	**Estimate Value :** a	0.671	0.667	0.664	0.672
	β	0.067	0.066	0.066	0.067
	Standard error : a	0.017	0.021	0.020	0.017
	β	0.0021	0.0027	0.006	0.0022
Random Effects	**Estimate Value :**ω_a	0.0719	0.0614	0.088	
	ω_β	0.0794	0.0735	0.1091	
	Standard error : ω_a	0.019		0.0624	
	ω_β	0.026		0.083	
Statistical Criteria	**-2 x log-likelihood :**	1756.60	1739.7	1758.108	1756.5
	AIC	1766.60	1751.704	1768.108	1766.5
	BIC	1768.11	1769.224	1769.621	1768.1
Execution time (s)		100	0.61	14.44	2.47

We can note that for all the methods, the estimation of the population parameters (fixed effect) are close. MONOLIX and NLMEFIT have values of the standard errors of the fixed effects, an indication of the reliability of the value, lower than the other tools, they estimated with more precision than suggested by NLME and SAEMIX outputs.

For the estimation of the random effects, MONOLIX seems to be the more accurate with standard errors of 0.019 and 0.026. The values of NLME are closest of MONOLIX's values but we can not check with the absence of a function returning the standard errors of the random effects.

The output of the *summary* function includes the values of the *Akaike Information Criterion (AIC)* and the *Bayesian Information Criterion (BIC)*used to compare models

with different numbers of parameters.

$$AIC = -2logLik + 2n_{par}$$

$$BIC = -2logLik + n_{par}log(N)$$

where n_{par} represents the number of parameters in the model and N the total number of observations.
NLME on R presents the lowest value of AIC, indeed it is preferable to have a model with the smaller AIC and BIC.

The Execution time shows the faster tools to estimate a nonlinear mixed-effects model. Monolix estimates a large time of 100 seconds of execution. NLME offers the quickest execution time with 0.61 second.

2.4.2 Interpretation of diagnostic plots

For better analysis of the goodness-of-fit of the model, it is necessary to have diagnostic plots as graphical analysis of residuals and predictions, distribution of the residual errors, random-effects parameters, ...
MONOLIX generates a wide variety of graphics that we will present following. MATLAB has the fewest options of plots for the analysis of the nonlinear mixed-effects models (Individual Fit, Population Fit, boxplot of the distribution of the random effects).

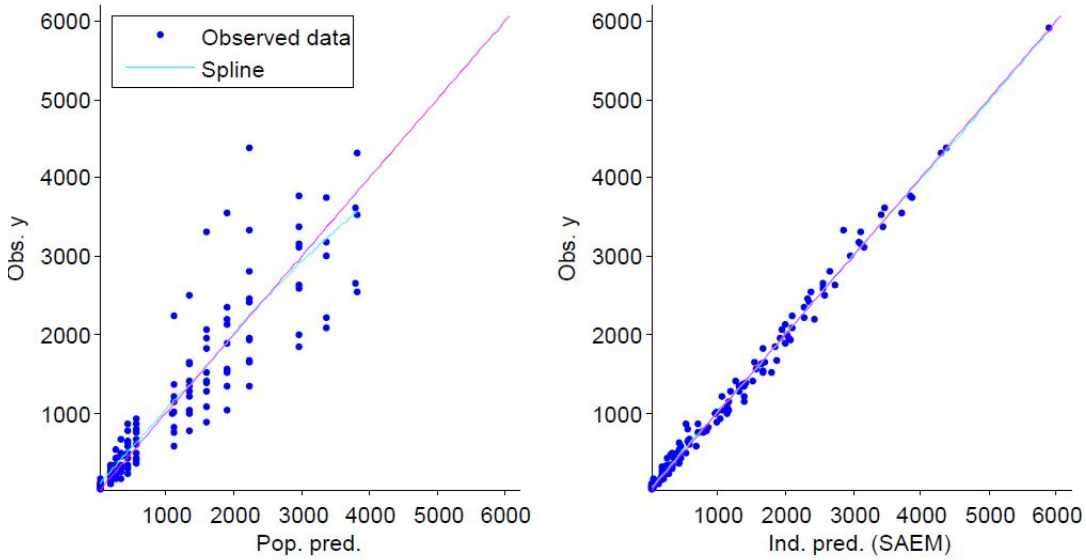

Figure 2: Observations vs Predictions on *Monolix*

The figure (2) presents observations versus predictions computed using the population parameters (on the left) and with the individual parameters (on the right).
Using the individual parameters, the scatter plot follows a linear curve ($y = x$) which means the predictions are highly similar to the observations. The displayed points using the estimated population parameters try to follow a linear curve. It is normal to note some dispersions because a population approach means to represent a general point of view of all individuals.

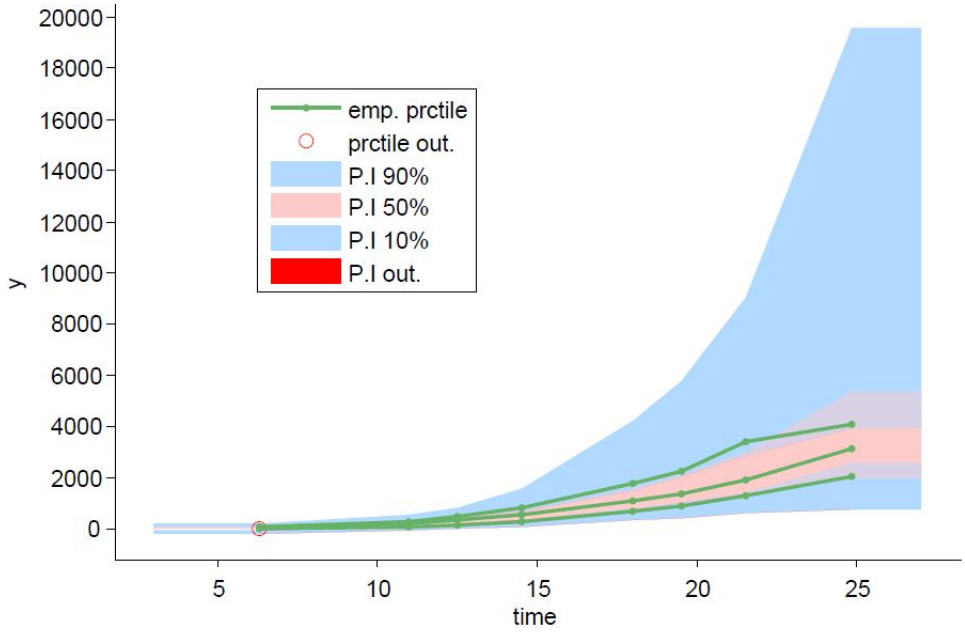

Figure 3: Visual Predictive Check on *Monolix*

The graphic (3) displays the Visual Predictive Check which summarizes the structural and statistical models by computing several quantiles of the empirical distribution of the data and the prediction intervals for these quantile are estimated. In the study of tumor growth in mices, the figure presents the VPC with the prediction interval for the quantiles 10, 50 and 90. The model is admissible because the quantiles of the empirical distribution are in the associated prediction intervals.

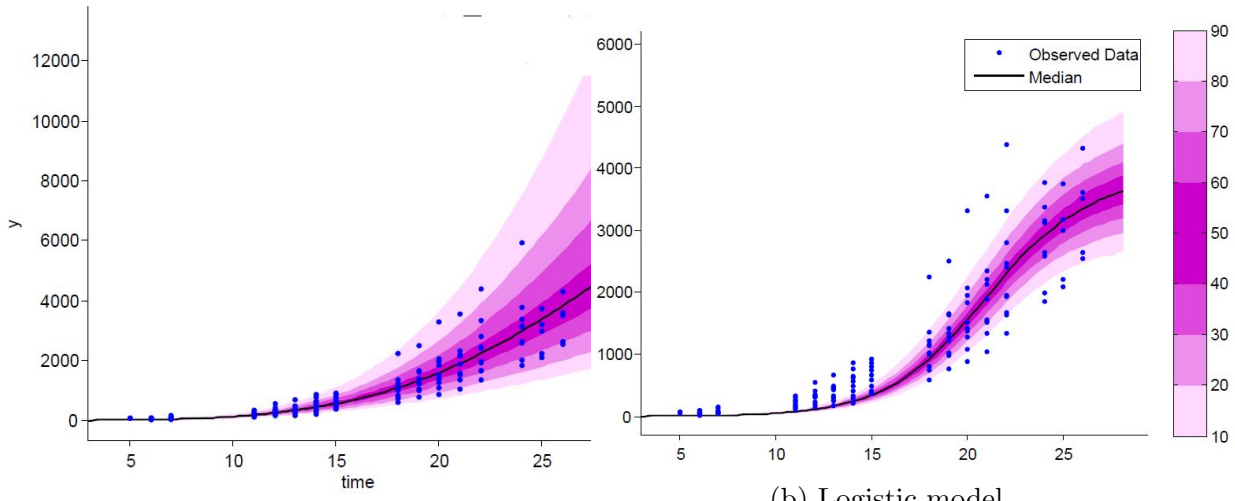

(a) Gompertz model

(b) Logistic model

Figure 4: Prediction distribution on *Monolix*

The figures (4) display the prediction distribution curves and allow to compare the observations with the theoretical distribution of the predictions. The black curve represents the population prediction median, the bands corresponding to the percentiles. Here, we varied the mathematical model to compare. On the left, it is the Gompertz model and on the right the Logistic model. The Gompertz model has a better prediction with the data than the other model.
The Logistic model is defined by :

$$\begin{cases} \frac{dV}{dt} = & aV(1-\frac{V}{K}) \\ V(t=0) = & 1\text{mm}^3 \end{cases}$$

where K is the carrying capacity which means the nutritional support that the tumor needs to grow.

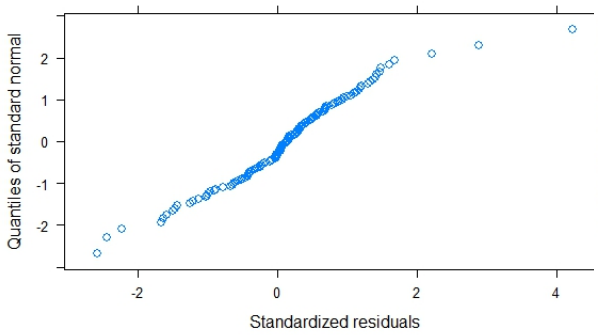

(a) Normal plot of residual with *NLME on R*

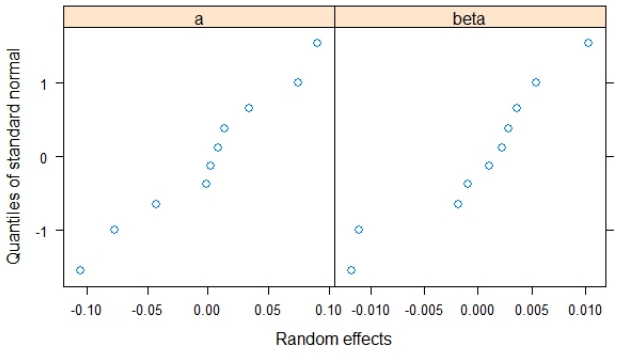

(b) Normal plot of random effects with *NLME on R*

The graphic on the left displays the normal plot of residual. The points follow a straight line which means the normality assumption of residual can be acceptable.

The second figure represents the normal plot of random effects. The assumption of normality for the random effects is reasonable.

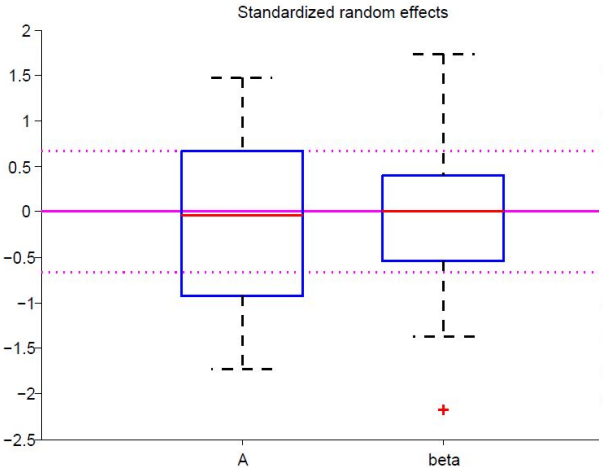

(a) Boxplot of the random effects on *Monolix*

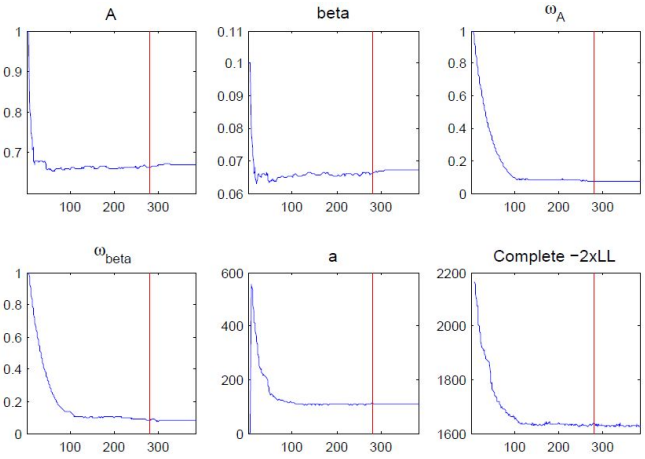

(b) Convergence SAEM on *Monolix*

On the left (a), it is a graph showing the distribution of the random effects on the population with boxplots for each parameters. The horizontal lines show the quantiles of a standard gaussian distribution. The distribution seems to be more expanded for the parameter a. For both, the mean is quite close of zero.

The figure (b) displays the convergence of the SAEM algorithm to estimate the parameters. For all the parameters, the convergence is quick, we can also reach the graphic with SAEMIX on R.

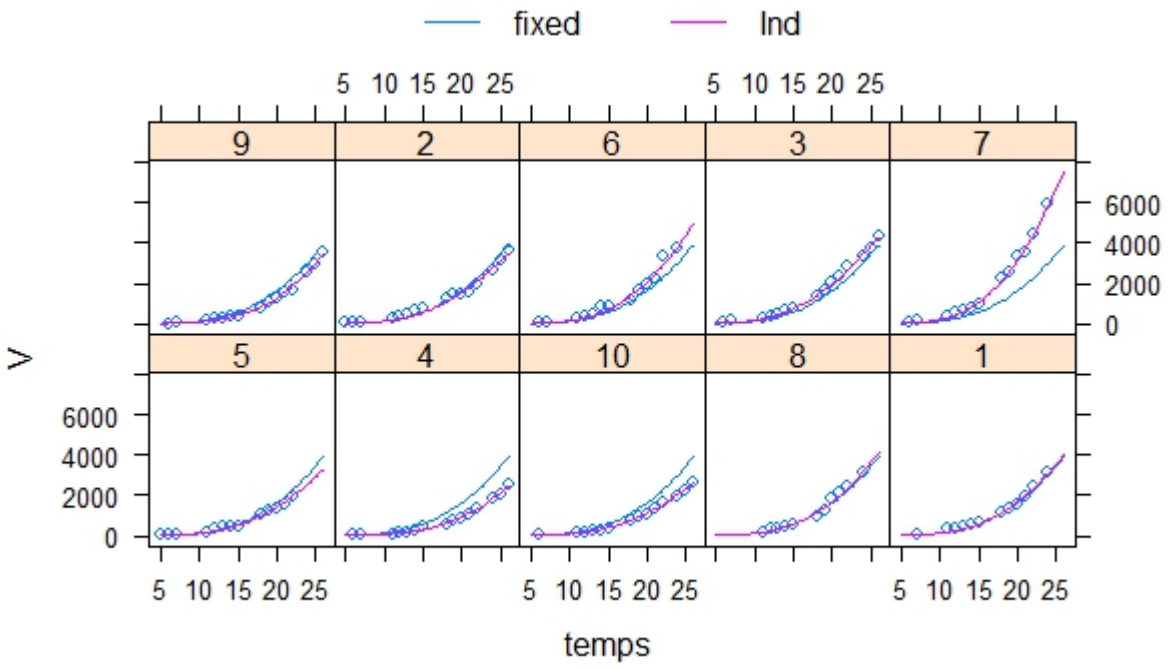

Figure 7: Population and Individual fits for each mouse NLME on R

This figure displays the population fit using the fixed effects, it is a typical curve for the population. The population fit represents a general look for all individuals. We can also note some variabilities between the population fit and the observations (for example the 4th or 7th mouse). Then, it is important to have individual parameters (random effects) distributed in the population which try to have a goodness-of-fit for each individual *(pink curves)*.

Conclusion

To conclude, the nonlinear mixed-effects model with the Gompertz structural model is well-suited to describe the general shape of the volume tumor growth for the population of 10 mice. Thanks to the random effects, each individual can also be described by a single model. Then, the nonlinear mixed-effects model is able to explain variability in the individual's curves.

We use an unique structural model to compare different tools for the analysis of mixed-effects models. MONOLIX is the most complete software, it gives us the necessary information for the study (estimated parameters, standard errors, statistical criteria, correlation matrix of the estimates). Nevertheless, it takes time to generate the results and the graphics because it has a wide choice of plots. Indeed, it lets us

more focus on exploring models and less programming with an ease of use.
The SAEMIX's outputs are the same as Monolix's but less precise.
NLME on R has the fastest execution time and it can be interfaced with Python. It also returns a lot of information like the confidence intervals on estimated parameters of the model and standardized within-group residuals except the standard errors of random effects. The possible plots are narrowest than Monolix's.
NLMEFIT on Matlab is accurate but the quantity of given information is very limited.

3 A mathematical model of two tumors in interaction

3.1 Discovery and assumptions of the concomitant resistance

Concomitant tumor resistance is a curious phenomenon by which the presence of a tumor (for example, a breast cancer) inhibits the growth of another implant (for example, in the lung), it trains a systemic (at the organism scale) growth suppression effect.
The first who described this phenomenon was Paul Ehrlich (1906) where he observed in mice bearing a growing tumor suppressed the growth of tumor cells inoculated at different sites.

Several hypothesis try to explain the concomitant immunity.
Paul Ehrlich (1906) assumed that two tumors competed for nutrients. Then, the first growing tumor would leave less nutrients for the other tumor growth (athrepsia : competition for nutrients).
The term "concomitant immunity" was introduced in reference to the Bashford's hypothesis (1908). For him, the growing of the primary tumor induced an anti-tumor immune response which failed to inhibit its progression. Nevertheless, the anti-tumor immune response could be effective in suppressing the second small tumor.
In 1972, DeWys studied this phenomenon and supposed that the primary tumor secreted inhibitory factors which suppressed directly the growth of the distant metastatic cells.
A similar assumption was formalized by Folkman in 1994 where he suggested that there was a systemic inhibition of the angiogenesis. That means the tumors release anti-angiogenesis factors in the organism which will slow the other tumor growth.
The angiogenesis traduces the situation in which the tumor attracts the blood vessels to get nutrients and to grow.

3.2 Experiments for the study of two tumors in interaction

Then, I worked during my internship around the study of [Benzekry et al., 2016] about the dynamics of concomitant resistance in which a mathematical model was established from experimental data obtained in collaboration with the Center of Cancer and Systems Biology at Boston, involving the two tumors growth inoculated simultaneously in the same organism.

Indeed, the experiments consisted in the simultaneous injection of two tumors of 10^6 Lewis Lung Carcinoma (3LL) cells in 10 mice. Tumor size was measured regularly over several days.

A statistical analysis of the volume data was performed to know if the differences in the increase of the tumors were significant or were due to natural variability in the tumor growth. Thus, the analysis involved control mice bearing single implants that we compared the growth with mice bearing two tumors.

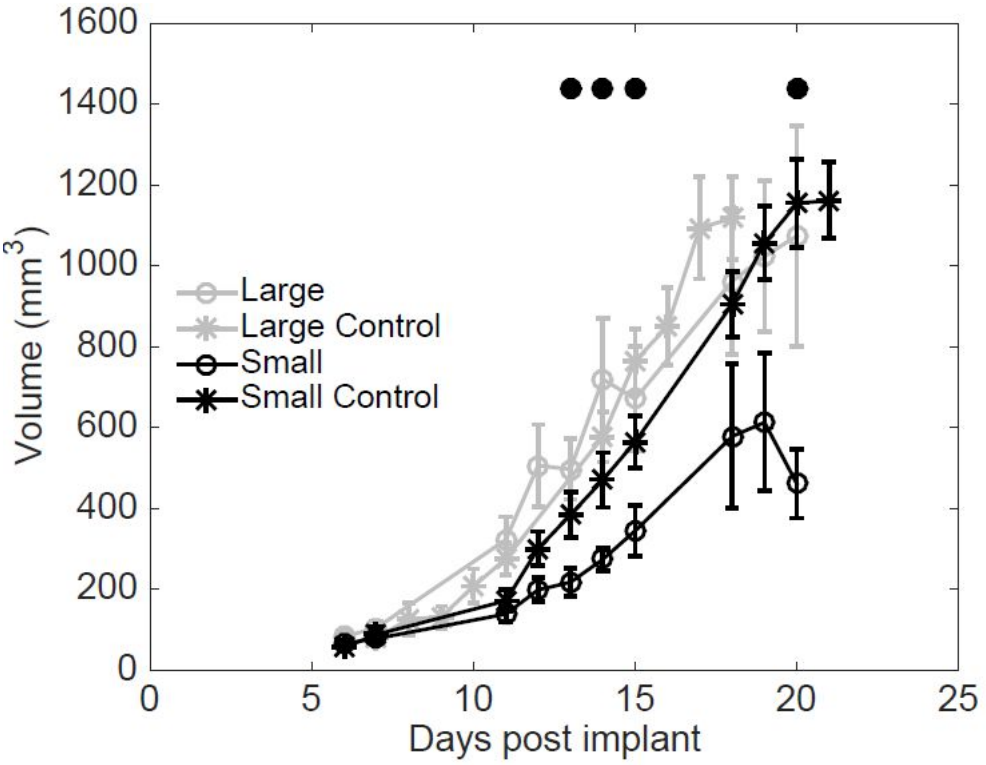

Figure 8: Volume of tumor data for control mice and mice bearing two tumors [Benzekry et al., 2016]

These results (8) shown statistically significant differences between the small tumors from mice bearing two tumors and the "small control" tumors.
Then, in a mice bearing two tumors, one tumor is growing normally which means at the same speed as a single tumor (Large and Small control), but the other grows significantly slower.

3.3 The mathematical model based on a theory explaining the phenomenon

[Benzekry et al., 2016] formalized a mathematical model from the theory of direct inhibition of proliferation to try to explain the phenomenon of concomitant tumor resistance, particularly the significantly slower kinetics observed in the small tumor in his

volume data of mice bearing two tumors.
The assumption of direct inhibition of proliferation consisted in the release of anti-proliferative factors from the tumor in the organism which will directly inhibit the growth of distant tumors.

The mathematical model which represents in a simple way this theory is defined by :

$$\begin{cases} \frac{dP_1}{dt} = & \alpha P_1 - (\beta P_1 + \gamma(P_1 + P_2))\mathbb{1}_{P_1>0}, & P_1(t=0) = V_{0,1} \\ \frac{dQ_1}{dt} = & \beta P_1 + \gamma(P_1 + P_2)\mathbb{1}_{P_1>0}, & Q_1(t=0) = 0 \\ \frac{dP_2}{dt} = & \alpha P_2 - (\beta P_2 + \gamma(P_1 + P_2))\mathbb{1}_{P_2>0}, & P_2(t=0) = V_{0,2} \\ \frac{dQ_2}{dt} = & \beta P_2 + \gamma(P_1 + P_2)\mathbb{1}_{P_2>0}, & Q_2(t=0) = 0 \end{cases} \tag{2}$$

Where :

- P_1, P_2 the proliferative cells of respectively the first and the second tumor
- Q_1, Q_2 the quiescent cells of respectively the first and the second tumor
- α the proliferation rate
- β the product of the production rate of anti-proliferation factors and the transfer rate from proliferation to quiescence
- γ the parameter representing the interaction between the two tumors (the tumor cells into the blood circulation)

Volumes of the two tumors at time t were denoted $V_1(t)$ and $V_2(t)$.
In this model, the population of tumor cells is divided between proliferative cells (P_1 and P_2) and quiescent cells (Q_1 and Q_2).

An assumption made on the experiments was the cell loss during the injection, where one tumor ($V_{0,1}$) had initially more cells than the other ($V_{0,2}$). Thus, it was fixed $V_{0,1} = 1\text{mm}^3$ ($\simeq 10^6$cells) and $V_{0,2} = 0.75\text{mm}^3$.

We note that the model is defined so that nothing happens if there is not proliferative cells (Heaviside functions).

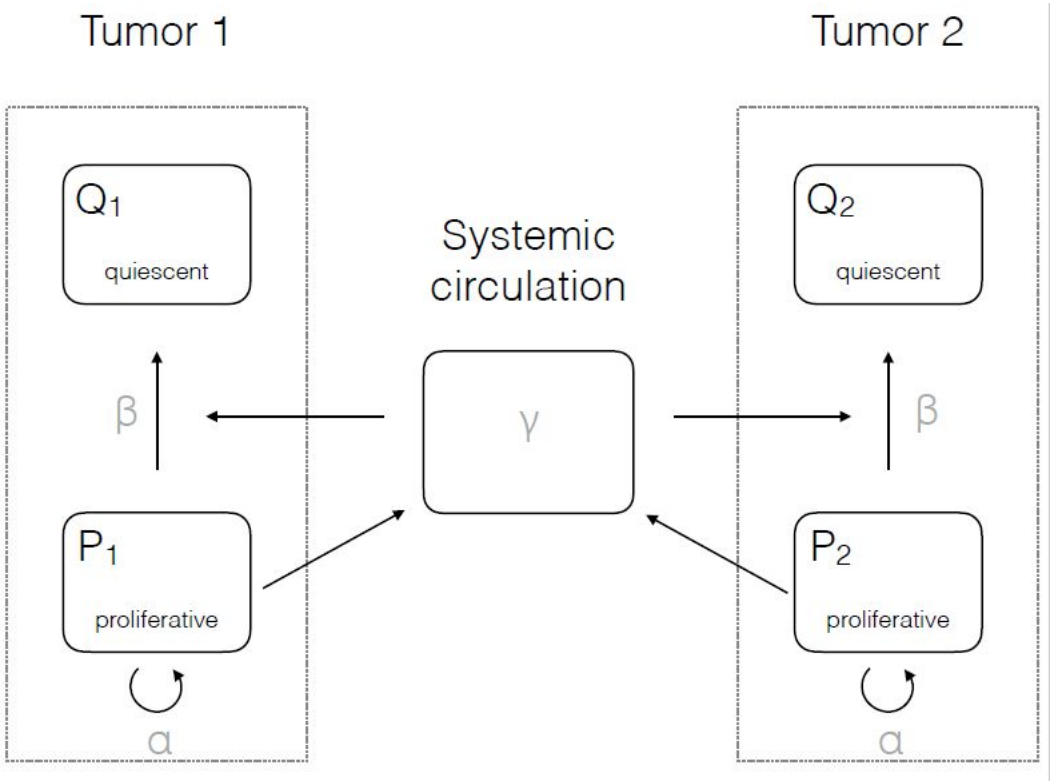

Figure 9: Simplified representation of the direct inhibition model [Benzekry et al., 2016]

The figure (9) summarizes and schematizes the role of the parameters involved in the mathematical model.

3.4 Results and goodness-of-fit of the model

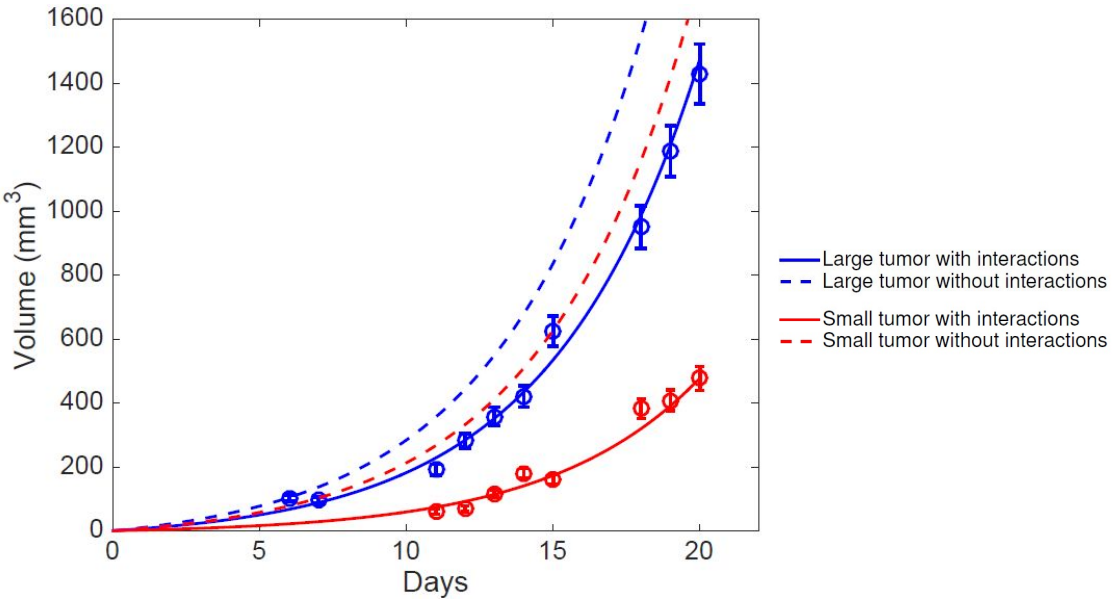

Figure 10: Fit on the two tumors data for a mouse and simulation without interaction ($\gamma = 0$) [Benzekry et al., 2016]

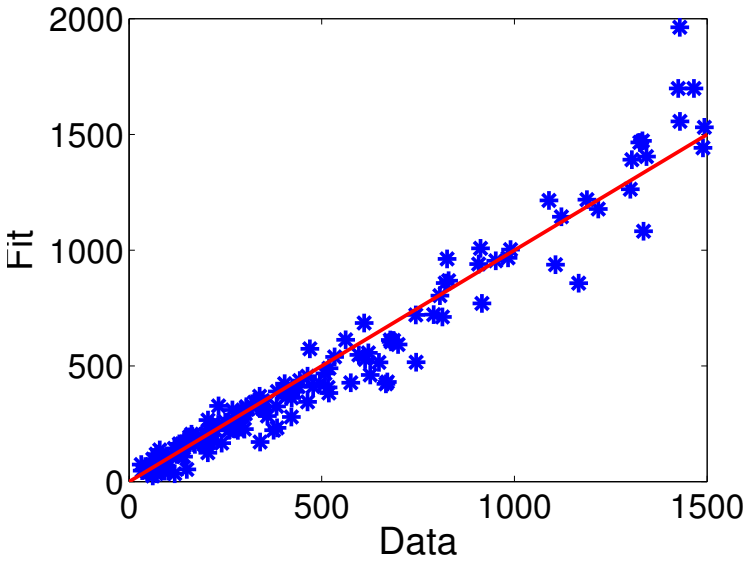

Figure 11: Fit vs data [Benzekry et al., 2016]

The model was fitted against the volume data of the two tumors in mice. The results (Fig. 10) shown a relevant goodness-of-fit, the model is able to fit the data very well

for each mouse.
Moreover, the prediction of the tumors behavior without the parameter of interaction γ permitted to confirm that the difference of the growth did not only come from the initial quantity of tumor cells inoculated but was also due to the potential interaction existing between the two tumors involved.
The good description was also confirmed by the figure (11) where the points of the fit versus the data follow a linear curve.

To understand the phenomenon of concomitant resistance, [Benzekry et al., 2016] investigated experimentally and theoretically. He formalized a mathematical model based on his experiments to try to represent the growth suppression of one of the two tumors in mice.
The model was constructed under the assumption of a direct growth rate decrease between the two tumors due to passage to quiescence, whose model's expression is simplified with only three parameters involved and identical for the two tumors. It also has a structural symmetry, indeed the inhibition effect is identical between the two tumors.
Moreover, its goodness-of-fit and identifiability of the parameters revealed to be satisfied and excellent. Then the model of direct inhibition of proliferation can explain the dynamics of concomitant resistance.

4 Confrontation of the two tumors model against others data

The goal of my internship was in a first time to improve the validation of the mathematical models defined in [Benzekry et al., 2016] which reproduce tumor growth, especially the Gompertz model and the direct inhibition of proliferation in two tumors model constructed from pre-clinical experiments.
For that reason, we test the mathematical models against independent data present in the scientific literature with Matlab.
In particular, we confront the models with [Gorelik et al., 1981] results which display several cases that we attempt to reproduce in silico.

4.1 Report on Gorelik's research on the mechanism of tumor «Concomitant Immunity »

To understand the complex interactions existing between the primary tumor and its distant metastases, [Gorelik et al., 1981] investigated on:

- the inhibitory effect exerted by the primary tumor on a tumor graft, taking into account the size of the first tumor and the number of reinoculated cells
- the inhibitory effect manifested in immunosuppressed mice
- the degree of specificity of the inhibitory effect

Conditions of the experiments : He used various sort of mice (immunocompetent or immunodeficient mice) and several kinds of tumors (Lewis Lung cacinoma 3LL, melanoma B16, lymphoma EL4, T-10 tumor, Madison lung carcinoma M109) to analyze the mechanism of concomitant immunity.
For his experiments, mice were inoculated subcutaneously with tumor cells (primary tumor) and when the tumor reached a certain size, mice were reinoculated intra foodpad with other tumor cells (second tumor graft).
We assumed that the relationships between the first tumor and the second tumor graft might reproduce the relationships existing during the growth of a primary tumor and its distant metastases.
The encountered difficulties during the experiments was mice might die from the first tumor before the develops to a visible second tumor. On the other hand, the introduction of high cell doses of the inoculated second tumor may modify the effect of concomitant immunity.

Influence of the size of the first tumor and number of reinoculated cells : The first series of experiments was to analyze the influence of the size of the growing first tumor and the inoculum size.

The first results shown that the inhibition of the growth of the second tumor depended on the size of the first tumor. Indeed, for the same number of reinoculated tumor cells, the second tumor was more inhibited when the mice had larger primary tumor.

In a second time, we can note that for the same volume of the primary tumor, the size of the second tumor can influence the inhibition. Indeed, for mice bearing tumors larger than 2cm in diameter, the growth of the reinoculated tumors is more suppressed when the quantity of injected tumor cells is smaller.

Then, these results demonstrate that the inhibitory effect is a function of the size of the tumor and the initial inoculum size.

Influence of the immune response : The next series of experiments were to study the involvement of the immune system in the concomitant immunity.
He tested the inhibitory effect in immunosuppressed mice (B mice or BALB/c mice) and in normal immunocompetent mice (normal mice or BALB mice) by varying the size of the tumor and the inoculum size.
In both experiments, the growth of the second graft in normal and in immunosuppressed mice was suppressed even completely arrested in some cases.

Moreover, we noted that after the surgical removal of the primary tumor, it occurred an augmented growth of metastases. Gorelik observed this spread with different immunosuppression procedures (Irradiation, Splenectomy,...).
The results shown that the inhibitory effect has a nonimmune component because in immunosuppressed mice, we observed the metastatic growth was more accelerated following removal of the local tumor, compared with normal tumor-bearing mice.

The concomitant immunity is not a result of specific immune response. Both immunological and non-immunilogical mechanisms might be involved in suppression of metastatic growth.

The specificity of the inhibitory effect : Gorelik repeated his experiments with tumors which differs in their growth characteristics to test the specificity of the inhibitory effect by varying the initial doses of tumor cells to reach a certain size of the tumor.
Indeed, in his previous study [Gorelik et al., 1978], he assumed that the inhibition of

metastatic growth is a tumor-specific phenomenon because his experiments reinoculating 3LL tumors cells was effective in the arrest of the accelerated metastatic growth, but not with EL4 and B16 tumors.
Nevertheless, these results shown that the suppression of growth of a second tumor seems to be tumor-non-specific. He observed an inhibition of the inoculum tumor cells whatever the first or the second tumor involved. This previous hypothesis may be attributed to the high growth rate of 3LL reinoculated tumor cells involving a stronger inhibitory effect.

To conclude,[Gorelik et al., 1981] discovered that the primary tumor cells produced inhibitory factors which suppressed the proliferation of second inoculum tumor cells. This inhibition was non-tumor-specific and not specially dependent of the immune response.
This inhibitory effect was also function of the size of the local tumor and the size of inoculum cells, indeed it appeared only when the first tumor reached a certain size.
Then, following removal of the primary tumor, without the inhibitory factors, the metastases accelerated their growth.
Moreover, other studies explained that tumors may have an antiproliferative effect in normal tissues.

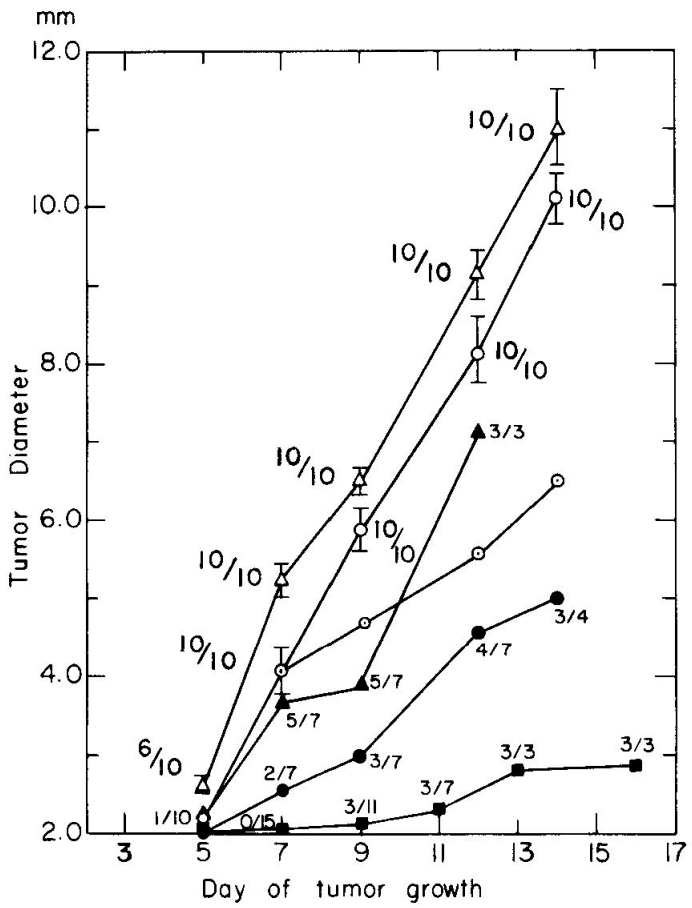

Figure 12: Suppression of the development of a second tumor cell inoculum transplanted into tumor-bearing mice [Gorelik et al., 1981]

Thanks to this study, we have available several tumor growth curves that we can use as data to fit with the model by modifying it to reproduce the Gorelik's experiments. However, the model has limits, it does not permit to simulate all the experiments available, for example we can not distinguish in the model the tumor growth in immunosuppressed mice or in normal mice.
Then, we selected the data from the Gorelik's article present on (Fig. 12) which involved the volume data of the second tumor measured over the time and reinoculated 10 days after the first implant (10^6 3LL cells) varying the quantities of 3LL cells reinoculated. The symbols represented : Normal non-tumor-bearing (control) mice inoculated with 5×10^5(△) or 2×10^5 (○) tumor cells ; mice bearing a 3LL tumor reinoculated with 5×10^5(▲) or 2×10^5 (●).
The observations shown that the inhibition of the growth of the second tumor was correlated with the initial reinoculum size.

4.2 Comparison of single tumor growth

First, we focus on a single tumor growth in normal mice inoculated intra footpad with different quantities of Lewis Lung Carcinoma (3LL) tumor cells (1×10^6, 5×10^5 or 2×10^5).
Moreover, from [Benzekry et al., 2016] we have 20 control mice bearing a single 3LL tumor with an initial value of 1×10^6 in their organism.

4.2.1 Gompertz model

The Gompertz model, whose equation expression is (1), exhibited a relevant goodness-of-fit and gives us a set of 20 parameters that we used to compare a single tumor growth with the data from [Gorelik et al., 1981].

Results

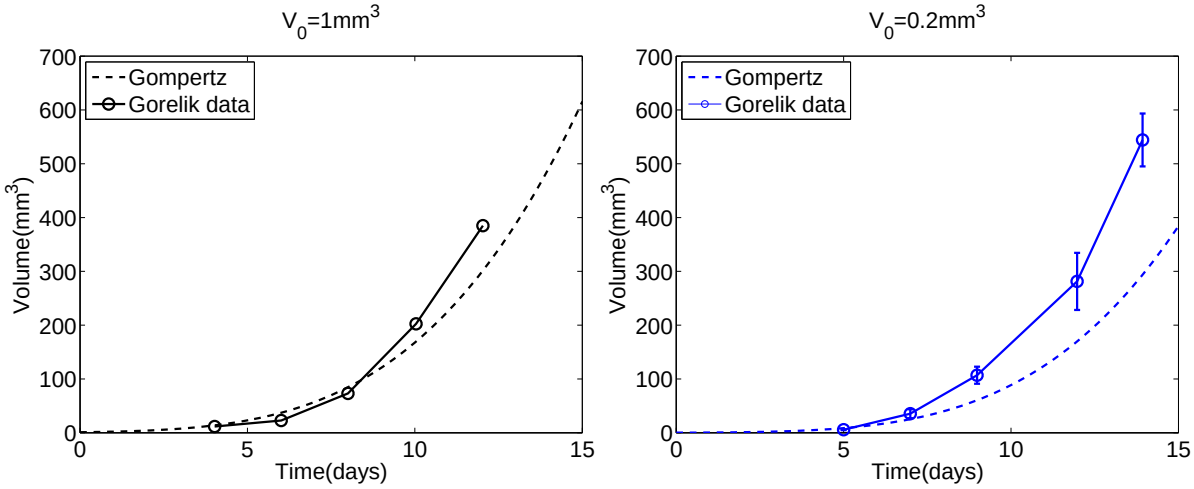

Figure 13: Simulation of tumor growth with Gompertz model

These plots which return Gorelik's data and the mean of the 20 Gompertz model simulations with an initial value of 1×10^6 or 2×10^5 tumor cells, show that the curves have the same behavior and similar values.
Globally, the single tumor model predicts correctly the tumor growth from Gorelik's experiments even if it seems to increase slightly slower than in reality when predicting tumor growth kinetics with a different initial tumor cells load (0.2mm^3) and using the parameters inferred from fitting the independent data set from [Benzekry et al., 2016].

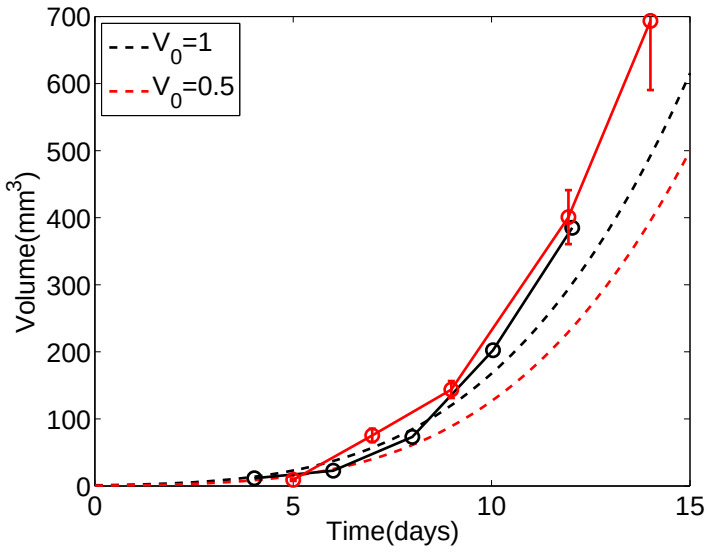

Figure 14: Tumor growth in control normal mice with Gompertz model

On the Fig 14, it is surprising that the tumor growth in Gorelik's data is similar injecting a tumor volume of 1mm^3 or 0.5mm^3.
The model can not represent well this phenomenon. Indeed, the initial condition influences the tumor growth in the Gompertz model due to the expression of the solution. The larger the number of implanted tumor cells, the faster the tumor grows.

4.2.2 Comparison with the Quiescent model

We can also compare the Gompertz model with another named Quiescent model which separates the tumor cells between proliferative factors P and quiescent factors Q.

The model is defined by :

$$\begin{cases} \frac{dP}{dt} = & \alpha P - (\beta+\gamma)P \\ \frac{dQ}{dt} = & (\beta+\gamma)P \\ P(t=0) = & V_0 \\ Q(t=0) = & 0 \end{cases} \tag{3}$$

whose solutions are :

$$\begin{cases} P(t) = & V_0 e^{(\alpha-\beta-\gamma)t} \\ Q(t) = & \frac{V_0(\beta+\gamma)}{(\alpha-\beta-\gamma)}(e^{(\alpha-\beta-\gamma)t}-1) \end{cases}$$

Results

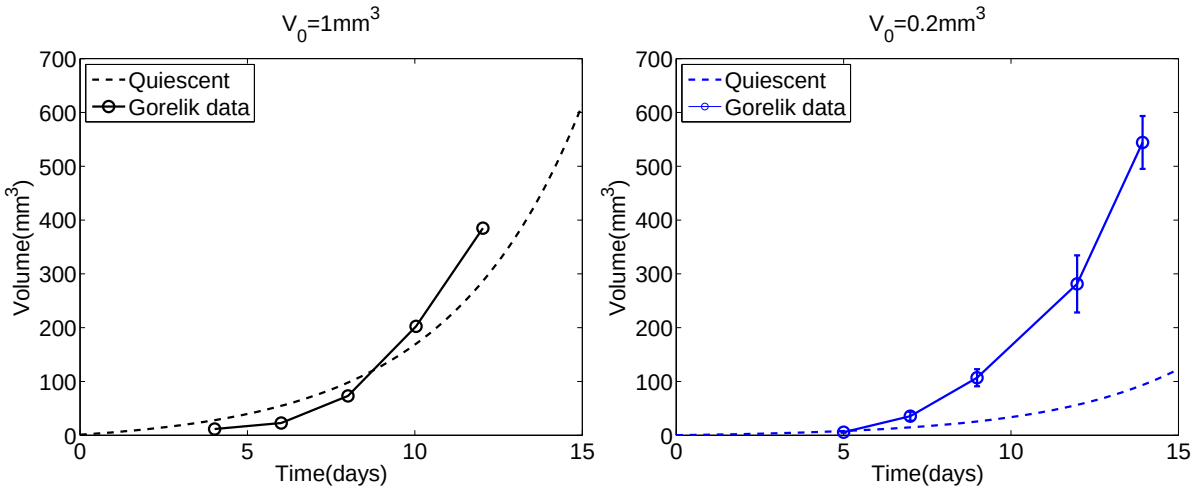

Figure 15: Simulation of tumor growth with Quiescent model

Thanks to the fits obtained here, the quiescent model has a good prediction of the data for $V_0 = 1\text{mm}^3$ which is the same initial condition than the experiments of the 20 mice. Nevertheless, we observe that it does not reproduce the Gorelik's experiment with an initial injection of $V_0 = 0.2\text{mm}^3$ because the quiescent curve on the second graph is far from the data and grows slower. The model is more sensitive to the initial conditions than the Gompertz model.

Therefore, the Gompertz model which was used and fitted for the experiments of the 20 mice [Benzekry et al., 2016] reproduces well independent and external data. It also has a better prediction of the general tumor growth than the Quiescent model which is very influenced by the initial conditions.

4.3 Test of the two tumors model against Gorelik's data

Second, we want to reproduce the Gorelik's experiments involving the data reached from Fig.(12). Hence it is interesting to simulate this reinoculation, the impact of the first tumor thanks to the two tumors tools that we will need to modify and to compare the results.

4.3.1 First simulation test

We recall that in [Benzekry et al., 2016] report, we have volume data of tumors measured over several days for 10 mice inoculated by two simultaneous 3LL tumor implants with $V_{0,1} = 1\text{mm}^3$ and $V_{0,2} = 0.75\text{mm}^3$.
We fit these data with the model of direct inhibition of proliferation whose equation (2) is expressed in the part 3. of the report, known for its goodness-of-fit which represents the interaction between two tumors in which a tumor produces inhibitory and proliferating factors.
Then, thanks to the 10 parameter sets reached following the fitting, we can simulate the Gorelik's experiment adapting the model.

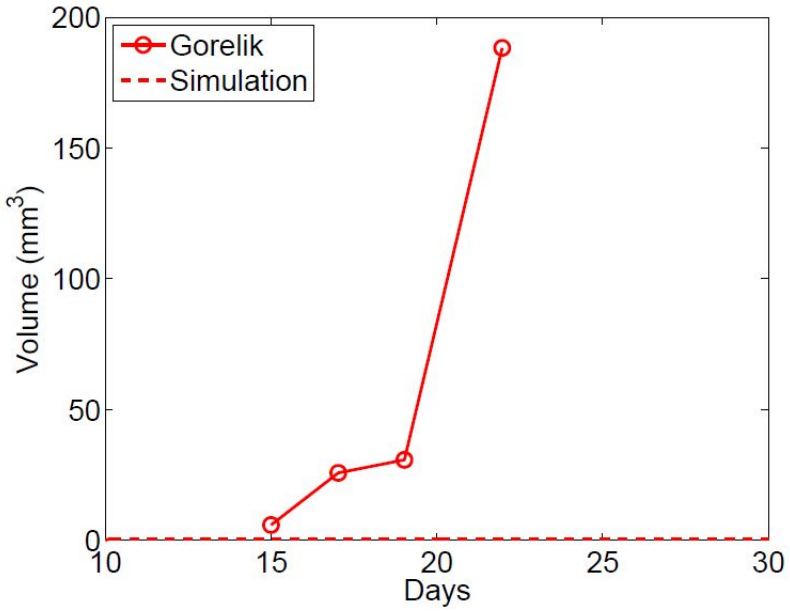

Figure 16: Simulation of the second tumor growth with 10 days after the first implant

These graphs display the second tumor growth simulated with a set of parameter obtained directly from [Benzekry et al., 2016] and added 10 days after the first inoculation of the primary tumor at $t = 0$ with $V_{0,1} = 1\text{mm}^3$ corresponding to 1×10^6 tumor

cells.

We observe that regardless of the set of parameters, the second tumor rapidly saturates and becomes constant. This can be explained by the small quantity of tumor cells $V_{0,2}$ (5×10^5 or 2×10^5 tumor cells) implanted at a time T_0 where the first tumor volume $V_1(T_0)$ is very important.
Indeed, the quantity of proliferative cells P_2 is not enough compared to the inhibition P_1 ($P_2 << P_1$) which will quickly exhaust the proliferative factors until the value 0.

Therefore, the two tumors model can not predict well this phenomenon of small tumor's reinoculation with the parameters obtained thanks to the fits of previously volume data.

4.3.2 Second simulation test

An other way to try to reproduce and to get closer to Gorelik's volume data is to start with his data and to fit them thanks to the direct inhibition model. The new returned parameters will allow us to simulate the phenomenon.

New set of parameters reached using volume data of the second tumor

In a first attempt, we fit the model on the volume data of the second tumor in normal tumor-bearing mice. We let the model adapt itself for the primary tumor volume behavior given the initial volumes and the day T_0 of the reinoculation.

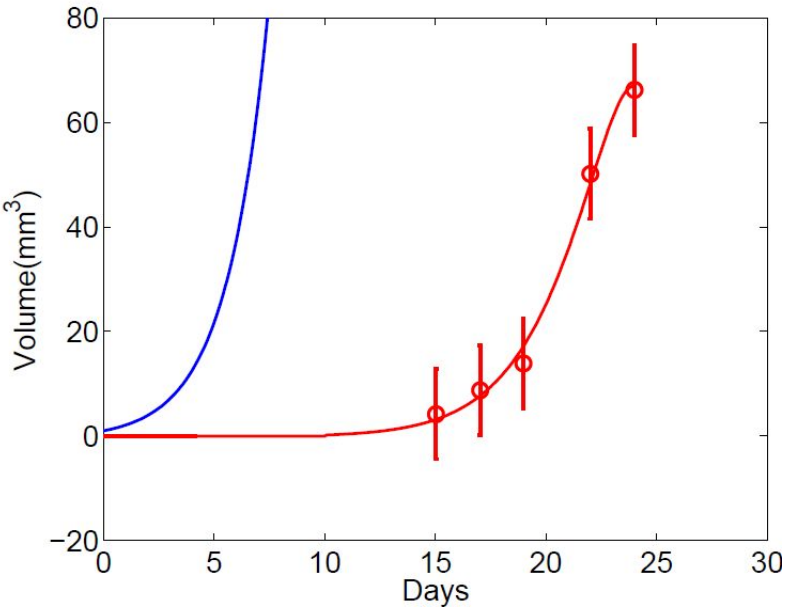

Figure 17: Fitting on the second tumor data in mice reinoculated with 2×10^5 tumor cells

We have a goodness-of-fit in the mice reinoculated with 2×10^5 tumor cells (Fig 17.), we can also observe on the graph the blue curve which represents the first tumor growth that the model adapts itself.
Moreover, the parameters γ are approximately close to 0 which means the model fits considering few or any interaction between the two tumors which is easier to adjust independently the second tumor.

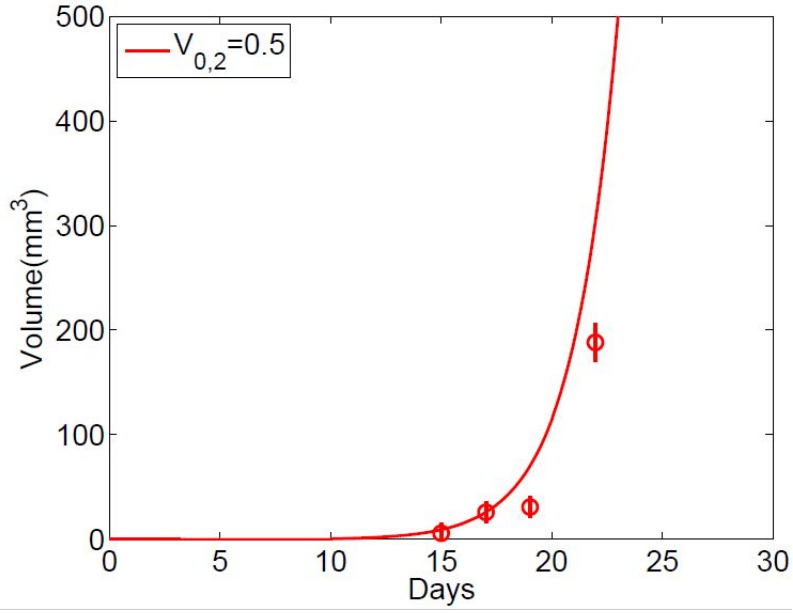

Figure 18: Prediction for a reinoculation of $5 \times 10^5 cells$

We adapt the direct inhibition model to simulate the Gorelik's experiment following his steps with the parameters obtained.
On the Fig 18., we use the parameters' set of the fit in mice reinoculated with $V_{0,2} = 0.2\text{mm}^3$ whose the goodness-of-fit is relevant (Fig 17.) to predict the second tumor growth with an initial second tumor value of 0.5mm^3.
The plot shows an appropriated simulation and predicts quite well the data. Indeed, for the same volume of the primary tumor, the size of the second tumor can influence the inhibition.

Then, we wonder what is the behavior and the dynamic of the primary tumor since the model fits without having any information about it.
We compare it with other tumor growth descriptions.

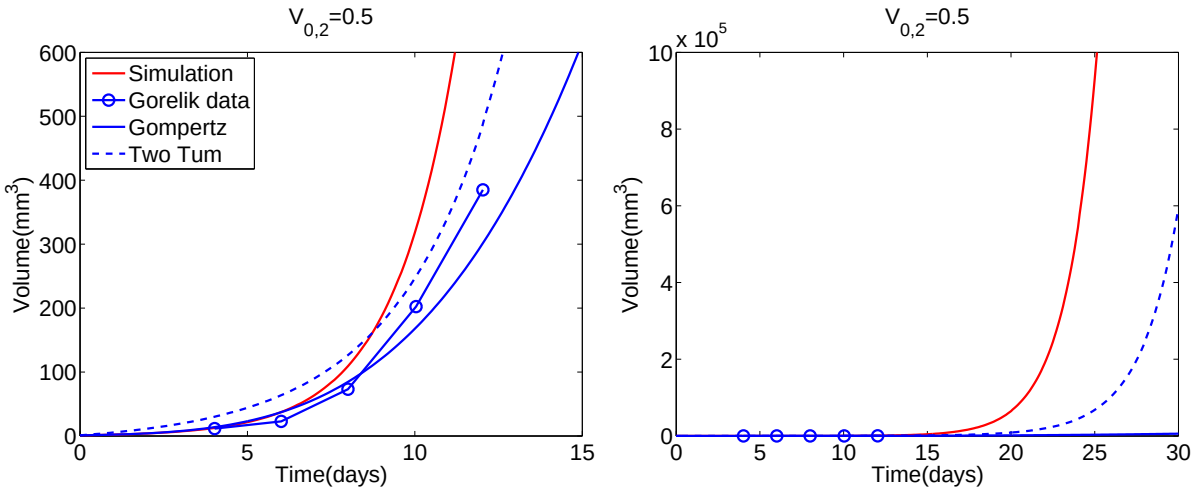

Figure 19: Primary tumor growth curves

These graphs display the primary tumor growth curves of our simulation with the previously parameters, Gorelik's data from his article, control mice simulated by the Gompertz model (Fig 19.) and with the first two tumors simulation.
At the beginning, the plot seems to comport as the others and follows well the Gorelik's data and the Gompertz prediction.
Later in time, the primary tumor increases faster than the other plots and attains high values (10^6mm^3) but keeps the same dynamic than the two tumors simulation.
Globally, the behavior of the primary tumor with the parameters reached with these data is possible.

Use of local and second tumor data for the simulation

We also try to fit the data taking into account the control mice curves inoculated with 1×10^6 tumor cells as the behavior of the primary tumor.

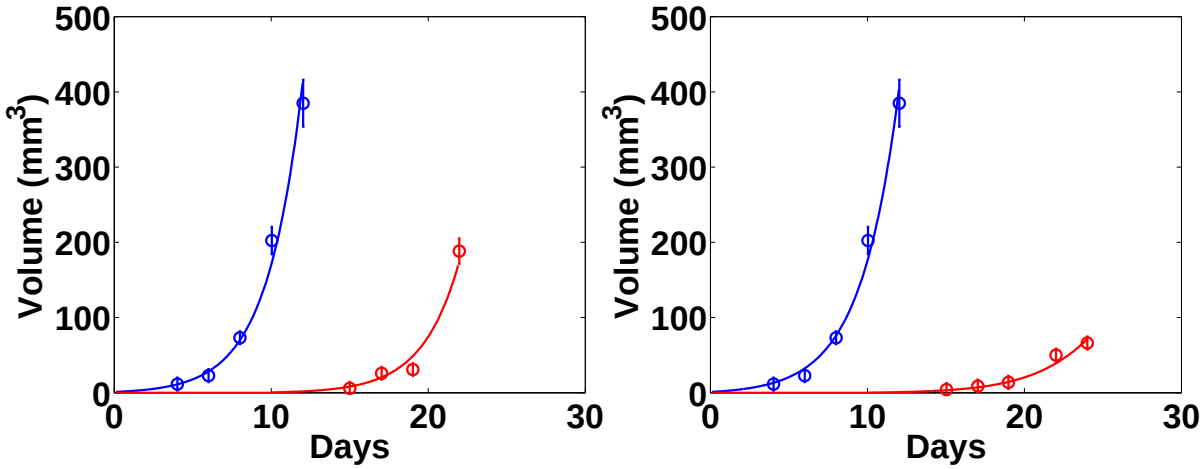

(a) $V_{0,2} = 0.5\text{mm}^3$ (b) $V_{0,2} = 0.2\text{mm}^3$

Figure 20: Fitting on volume data of control mice inoculated with 1×10^6 3LL and on second tumor data in mice reinoculated 10 days later with $V_{0,2}\text{mm}^3$ of 3LL

To adjust the best, we search manually the initial parameters which allow a good description of the data.
Then, the two tumors model have a goodness-of-fit and adjust well the data of the primary and the second tumor (Fig 20.).
We use the parameters obtained where γ value is low, to predict the experiments of Gorelik.

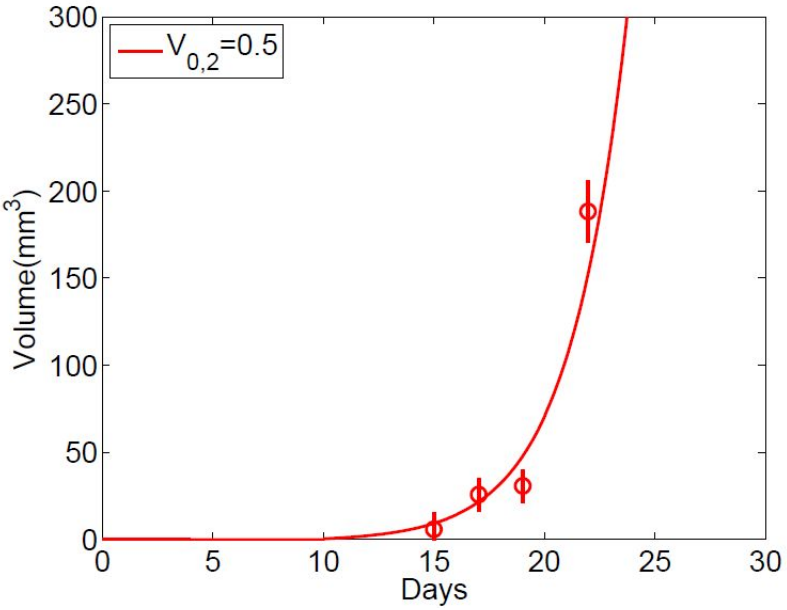

Figure 21: Prediction for a reinoculation of 5×10^5 tumor cells

We use the parameters obtained to simulate and try to predict the data.
On the Fig 21., taking the parameters of the fit in mice reinoculated with $V_{0,2} = 0.2\text{mm}^3$ (Fig 20,b.), the red graph shows that we predict well the second situation where mice are reinoculated with $V_{0,2} = 0.5\text{mm}^3$.

Therefore, the two tumors model based on the experiments from [Benzekry et al., 2016] can not reproduce the reinoculation of a second tumor with the existing parameters. Indeed, the large size of the primary tumor completely inhibits the growth of the second tumor which saturates quickly with these parameters.
An other way is to use the data from [Gorelik et al., 1981] and to fit on to obtain new sets of parameters. The direct inhibition of proliferation model exhibits a relevant goodness-of-fit and allows a good prediction of Gorelik's experiments.

Conclusion

To conclude, whereas it was constructed from [Benzekry et al., 2016] experiments, the strength of the direct inhibition of proliferation model is to be able to fit and describe external and independent data, but also to predict different and varied situations. It may be possible that the biological variability of mice (due to the life conditions or the temperature,...) was involved in difficulties taking directly the parameters used from [Benzekry et al., 2016]. It is also interesting to note that the data we treat here have the same sort of tumor cells in the two studies : Lewis Lung Carcinoma (3LL).

5 Study on the acceleration of metastases' growth

What is the importance of the concomitant resistance ?

The importance of this phenomenon occurs following the surgical removal of the primary tumor where the suppression of the inhibition's strength leads to a dramatic acceleration of metastatic growth. These dramatic post-surgical consequences was find in some clinical cases which had cause death of patients.

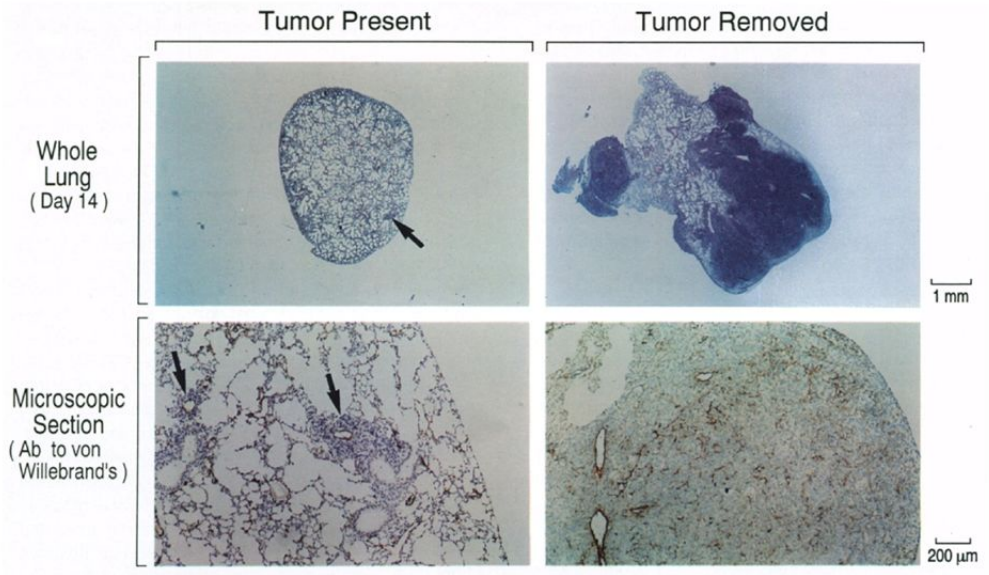

Figure 22: The presence of a Primary Tumor is Associated with an Inhibition of Neovascularization and Growth of its Metastases - *O'Reilly, Folkman et al., Angiostatin: A Novel Angiogenesis Inhibitor That Mediates te Suppression of Metastases by a Lewis Lung Carcinoma, Cell 1994*

The image (22) reflects well the impact of the surgical removal of the local tumor on metastasis. Indeed, on the left of the figure, the arrows point small metastasis presents in the mouse lung ; after that the tumor removed, on the right, we observe a metastatic explosion.

Hence an other part of my study internship was to modify the initial Matlab program ([Benzekry et al., 2016]) implementing the two tumors tools to simulate the surgical removal's impact and to quantify this acceleration.

5.1 Simulation of surgical removal

First, we modify the Matlab program taking the 10 parameters directly obtained from [Benzekry et al., 2016], to simulate the surgical removal of the first tumor by varying the day of excision (T_0). Then, we can test the effect of the ablation of the primary tumor on the development of the second.

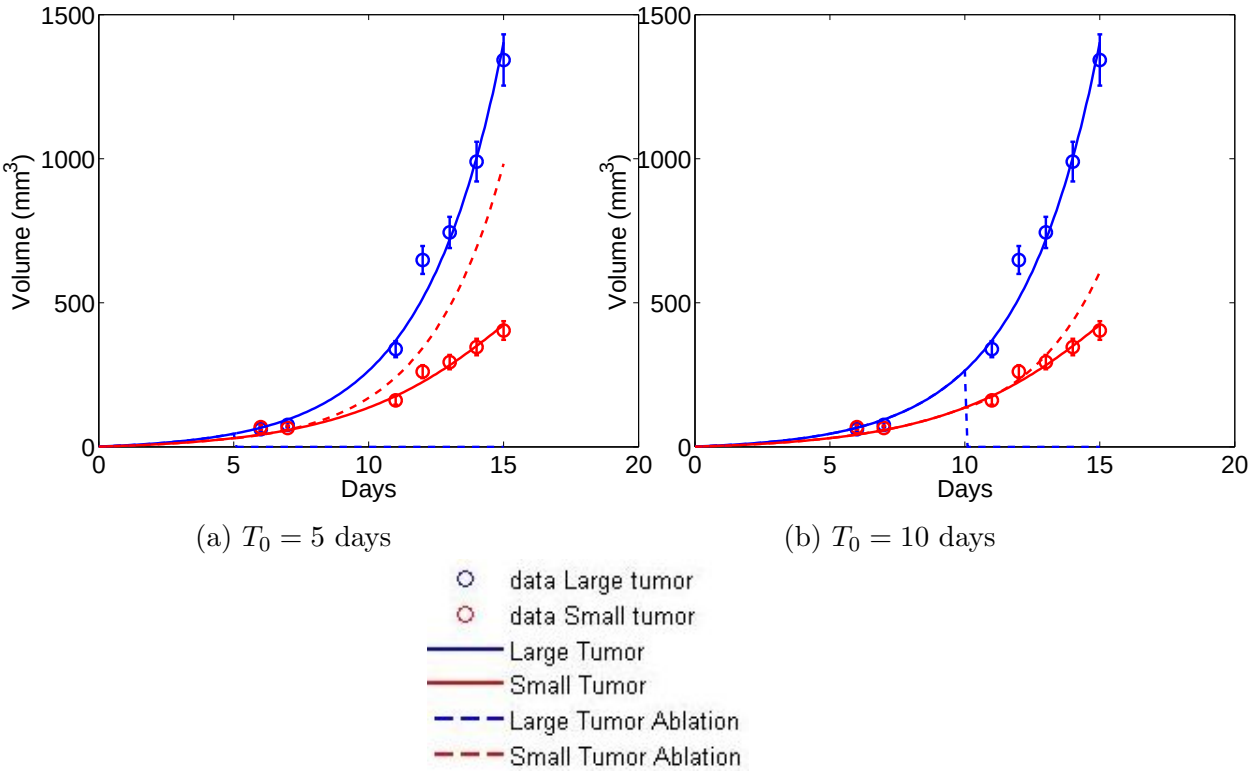

(a) $T_0 = 5$ days

(b) $T_0 = 10$ days

Figure 23: Ablation of the primary tumor at day T_0 after implant in mouse

These plots show well an acceleration of the second tumor growth following surgical removal of the primary tumors. The inhibitory effects from the local tumor to the second tumor are suppressed thanks to the ablation. The direct inhibition of proliferation model can represent the augmented metastatic growth.

We can note that [Gorelik et al., 1978] also studied the effects of the local tumor's presece on the inhibition of metastatic growth, in particular the increase of metastatic growth following the removal of the primary tumor.
He tested the effect of the ablation of the primary tumor (3LL tumor cells) induced in footpad in mice, on the development of lung metastases.
Following the amputation, he observed a dramatic increase of pulmonary metastases

growth (697mg against 231mg in non-amputated mice). Moreover, the ablation was following in all cases by severe dyspnea.

Then, this model which generates the inhibitory behavior of a local tumor on progression of metastases, also simulates the assumptions of Gorelik on the increase of metastatic growth following tumor excision.

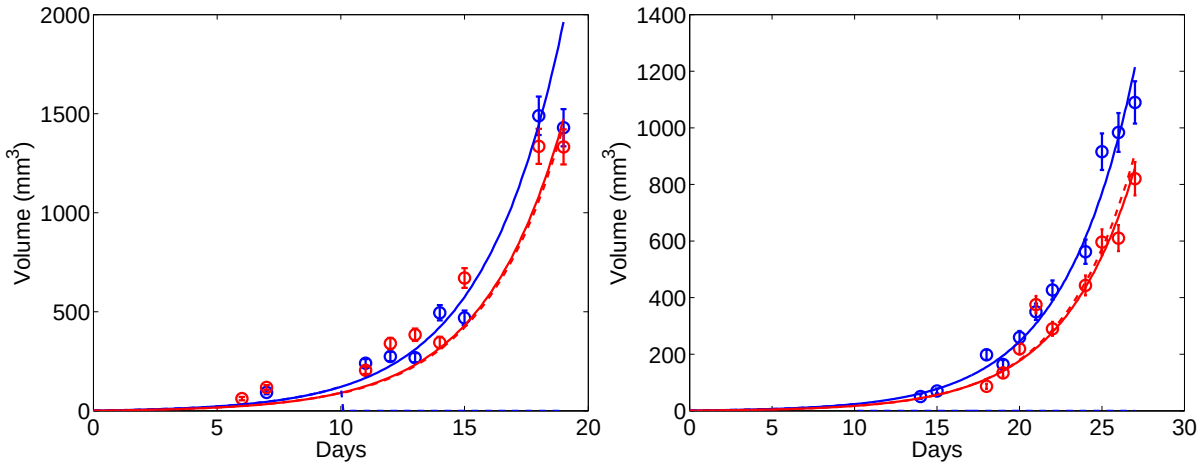

(a) mouse 2 (b) mouse 9

Figure 24: Particular cases - Ablation of the primary tumor 10 days after implant in mouse

Nevertheless, we have two particular cases were the phenomenon was not observable. Indeed, after the ablation of the primary tumor, the other tumor grows in the same way as without amputation. These plots don't indicate a significant increase of metastatic growth.
It is interesting to note that these cases occur in mice where a connecting blood vessel joining the two tumors were found in [Benzekry et al., 2016] experiments.

5.2 Quantify the metastatic acceleration

5.2.1 Method

After simulating the surgical removal of a local tumor in mice, we investigated on this metastatic acceleration to evaluate it according the day of the amputation or the volume of the excised tumor because each tumor grows differently. Indeed, we want to know if it exists a link or a dependence between them.

To quantify the increase of metastatic growth, we define in percent the acceleration by

$$Acc_{T_0,\tau}(\%) = \frac{V(T_0+\tau) - V_{ref}(T_0+\tau)}{V_{ref}(T_0+\tau)} \times 100$$

Where T_0 is the day of ablation, τ days after the excision, V_{ref} the fit of the second tumor without amputation, V the second tumor with ablation.

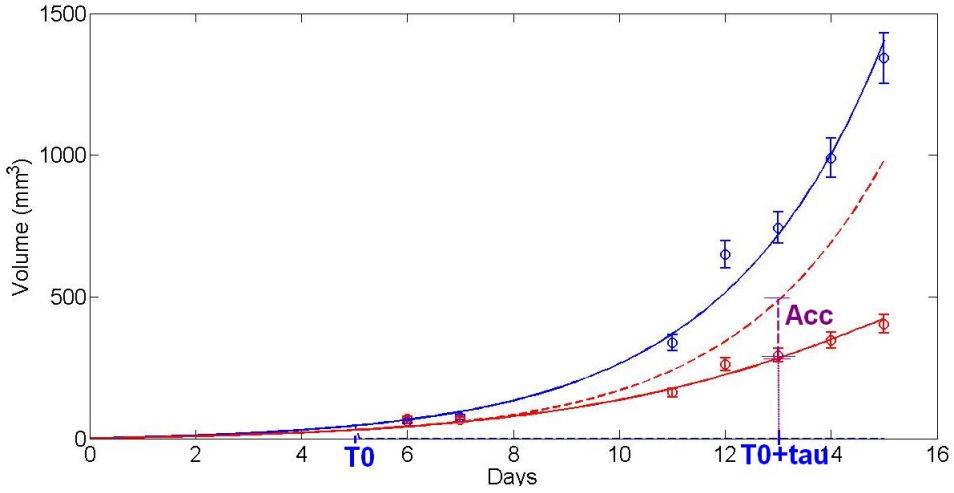

Figure 25: Acceleration of metastatic growth

5.2.2 Results

We summarize in a table the results of the acceleration in percent for some mice according the day of excision T_0 and the volume of excised tumor V_0.
We note that the acceleration vary for each mouse because the volume of tumors doesn't grow in the same way, for some it grows faster than others.

Mouse 4 :

T_0(days)	$Acc_{T_0,5}(\%)$	$Acc_{T_0,10}(\%)$
1	35.20	189.88
5	54.18	753.43
10	241.81	3351
13	82.83	1033.10
15	-3.97	-3.97

$V_0(mm^3)$	$Acc_{V_0,5}(\%)$	$Acc_{V_0,10}(\%)$
1	33.24	166.42
250	223.53	3489.7
500	308.93	3795.11
750	226.68	2775.14
1000	105.61	1252.64

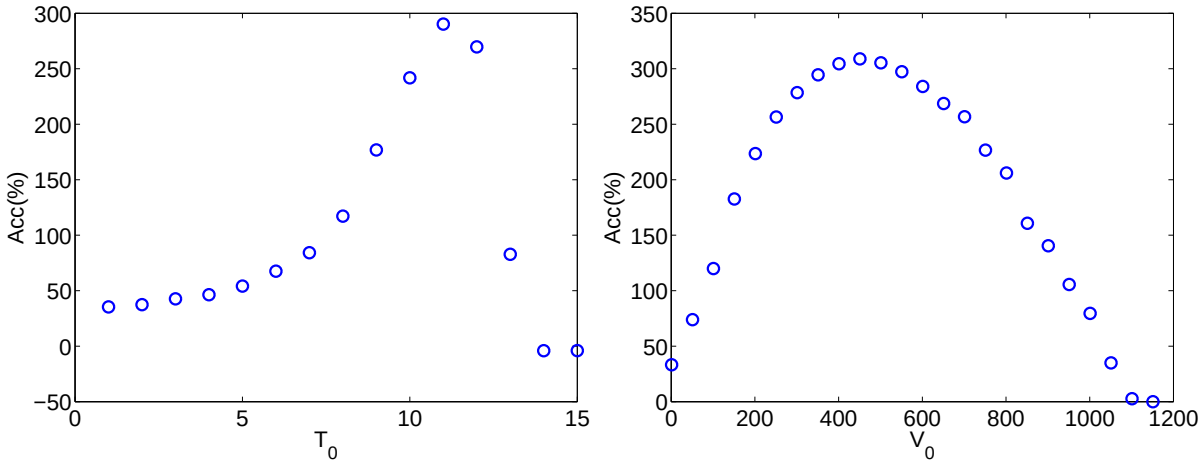

Figure 26: Acceleration in percent 5 days after amputation in mouse 4

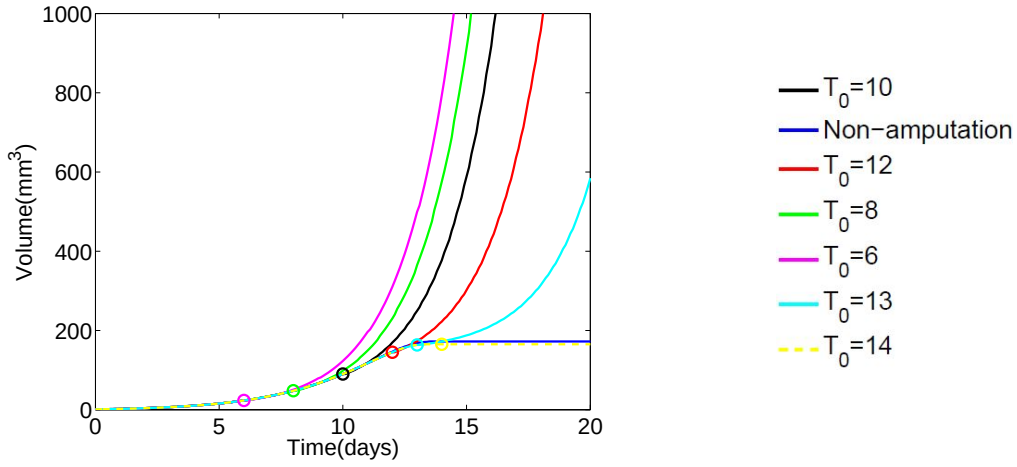

Figure 27: Volume over time for different T_0

Mouse 6 :

T_0(days)	$Acc_{T_0,5}(\%)$	$Acc_{T_0,10}(\%)$
1	28.10	123.76
5	34.89	277.96
10	92.52	948.96
14	89.81	656.04
15	-2.30	-2.30

$V_0(mm^3)$	$Acc_{V_0,5}(\%)$	$Acc_{V_0,10}(\%)$
1	27.74	115.28
250	57.62	714.22
500	98.89	1033.83
750	140.50	1157.63
1000	148.23	1165.39
1200	145.51	1100

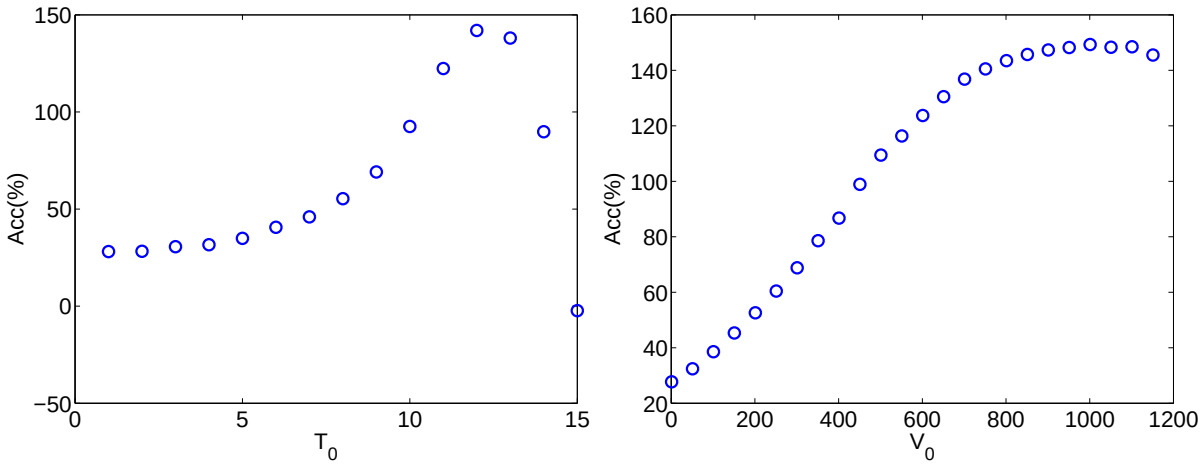

Figure 28: Acceleration in percent 5 days after amputation in mouse 6

Even if the acceleration grows more or less slowly depending on the mouse, these results which occur in 8/10 mice reveal acceleration's curves non-monotone which is quite surprising and non-intuitive.
Until a certain size of the local tumor V_0* (i.e corresponding to one amputation's day T_0*), the second tumor growth increases. Beyond this day, thanks to the plots, we observe a reduction of this acceleration.
Hence, that means until a volume of the primary tumor, the surgical removal can have dramatic consequences leading an augmented metastatic growth caused by the inhibitory effect suppression of the local tumor. If we wait long enough that a tumor reaches a certain size, the incidence of the amputation will be less important.

TABLE II

EFFECT OF SIZE OF LOCAL TUMOR AT TIME OF EXCISION ON THE INCREASE OF PROGRESSION OF LUNG METASTASIS [1]

Group No.	No. of mice	Treatment	Diameter of local tumor at time of amputation (mm)	No. of metastases per lung	Volume of metastases (mm^3)	Weight of lungs (mg)	Weight of spleen (mg)
1	9	Amputated	8-10	29 *	2.8±0.4 *	215±24 *	159±16 *
2	10	Amputated	6-9	19	4.1±0.8 *	248±22 *	163±5 *
3	10	Amputated	4-6	5 *	3.4±1.1 *	171±11 *	143±5 *
4	11	Non-amputated		11	0.4±0.09	141±7.2	325±42

[1] 1×10^5 3LL tumor cells were inoculated into the right footpad. Fifteen days later mice were divided into groups according to the diameter of their primary tumors. Nine days following excision of the primary tumor the development of pulmonary metastases was examined.

* Significantly different from group 4, $p < 0.05$.

Figure 29: [Gorelik et al., 1978] results on the increase of progression of lung metastasis

These observations were already been found in [Gorelik et al., 1978] experiments (see Fig.29) where he varied the size of the excised tumor to see the influence on the metastatic acceleration. The number of metastases was correlated with the size of the primary tumor whereas their volume increased ($3.4mm^3$ to $4.1mm^3$) and decreased ($4.1mm^3$ to $2.8mm^3$) when the size of the local tumor augments.

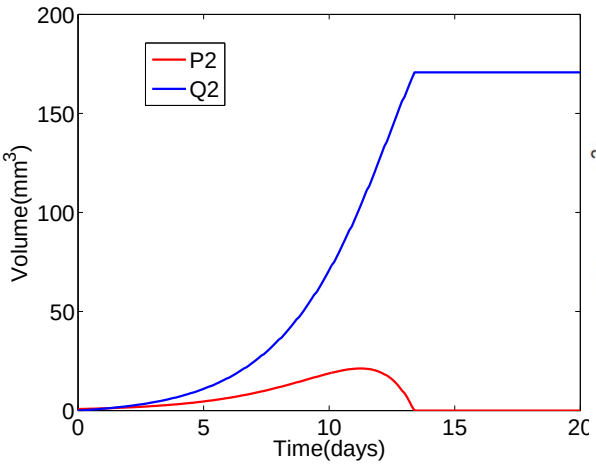

(a) Proliferative and Quiescent cells in the secondary tumor without amputation in mouse 4

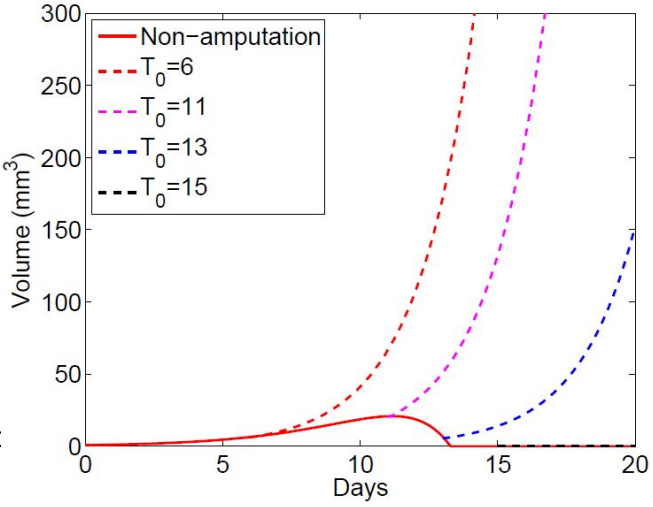

(b) Proliferative cells growth

The phenomenon found in the mice can be explained by the evolution of the proliferative and the quiescent cells in the secondary tumor. Following a certain date of

the amputation, the proliferative cells decreases may be due to the local tumor which reaches a big size and send a large quantity of inhibitory factors. Then, the metastatic acceleration's impact is less important because the quantity of proliferative cells is not enough compared to the inhibition ($P_2 << P_1$). Subsequently, following the excision of the primary tumor, the acceleration stays at the value 0 due to the depletion of P_2.

We recapitulate all the results in a general table.

$Acc_{T_0,5}(\%)$											
T_0	1	3	4	5	6	7	8	10	median	mean	std
1	4.31	14.29	35.20	11.14	28.10	9.36	18.29	21.05	12.72	13.75	12.36
5	3.81	14.01	54.18	9.97	34.89	8.67	18.88	24.13	11.99	16.49	17.53
10	4.69	18.80	241.81	11.91	92.52	10.56	28.60	42.53	15.35	44.99	74.57
15	5.41	32.01	-3.97	16.26	13.75	71.21	0.11	132.47	9.58	26.41	43.68
20	6.28	67.66	-2.35	29.03	-1.41	20.82	-1.08	-1.631	2.60	14.66	24.45
25	7.35	-0.74	-1.73	31.80	-0.94	45.11	-0.72	-1.07	-0.73	9.88	18.22
30	9.13	-0.36	-1.11	-0.27	-0.47	0.42	-0.34	-0.54	-0.35	0.81	3.39
$Acc_{T_0,10}(\%)$											
1	16.29	50.87	189.88	37.76	123.76	32.47	67.79	83.03	44.31	59.92	59.9
5	17.74	62.90	753.43	42.36	277.96	36.74	93.00	129.71	52.63	141.41	230.4
10	19.11	101.99	3351	55.09	948.96	45.59	225.15	449.94	78.54	519.82	1038.2
15	22.19	271.53	-3.97	94.82	67.44	485.92	2.76	1070.14	44.82	200.82	344.1
20	25.60	356.82	-3.12	202.45	-1.84	139.69	-1.43	-2.25	12.08	89.49	0.13
25	31.79	-1.14	-2.51	131.61	-1.37	302.63	-1.07	-1.69	-1.11	57.28	0.11
30	42.58	-0.76	-1.89	-0.56	-0.90	2.79	-0.69	-1.16	-0.73	4.92	0.02

$Acc_{V_0,5}(\%)$											
V_0	1	3	4	5	6	7	8	10	median	mean	std
1	4.25	14.58	33.24	11.59	27.74	9.53	18.60	20.81	13.08	13.49	12.04
250	4.00	21.35	223.53	12.73	57.62	11.41	25.91	40.55	17.76	43.29	77.44
500	4.65	31.89	308.93	15.81	98.89	14.02	39.85	62.94	24.83	58.50	93.31
750	4.70	47.82	226.68	19.14	140.50	16.42	60.12	90.15	33.48	60.20	74.22
1000	5.75	60.16	105.61	22.55	148.23	17.74	74.04	109.73	42.58	52.64	52.64
1500	5.87	70.04	0	31.21	116.74	22.56	82.24	140.42	50.63	58.64	52.13
2000	5.40	55.31	0	41.54	42.14	26.54	62.54	138.18	41.84	46.46	43.15
$Acc_{V_0,10}(\%)$											
1	17.17	50.96	166.42	38.58	115.28	33.22	66.76	80.16	44.77	56.72	52.9
250	20.12	166.55	3489.7	62.56	714.22	55.33	230.49	438.21	114.56	517.66	1069.2
500	20.45	288.62	3795.1	93.00	1033.8	73.61	381.37	722.70	190.81	640.80	1161.0
750	21.60	359.24	2775.1	132.90	1157.6	93.41	459.44	902.16	246.07	590.07	865.4
1000	22.42	387.04	1252.6	162.52	1165.4	109.64	492.16	998.89	279.34	431.78	453.5
1500	24.1	372.6	0	212.7	889.4	171.0	462.9	1089.8	292.63	402.81	398.0
2000	25.4	279.3	0	226.6	314.7	212.4	346.6	1034.5	252.99	304.95	320.9

Even if the experimental conditions attempt to reduce the variability, these results present high variations with important values of the standard deviation. Indeed, the organism where the tumors grow or the life conditions is different for each mouse and may interfere in the findings.

Mouse 2 :

T_0(days)	$Acc_{T_0,5}(\%)$	$Acc_{T_0,10}(\%)$
1	-3.18	-3.45
5	-2.61	-1.64
10	-1.31	-1.28
15	-0.80	-0.30

$V_0(mm^3)$	$Acc_{V_0,5}(\%)$	$Acc_{V_0,10}(\%)$
1	-3.79	-2.79
250	-2.88	-2.44
500	-2.43	-2.57
750	-2.76	-2.64
1000	-2.77	-2.06

We also note for 2 mice that their accelerations $Acc_{T_0,\tau}$ and $Acc_{V_0,\tau}$ are very weak and stay approximately constant close to 0. Moreover, the small variation may be due to the numerical error in the resolution of the ordinary differential equation with Euler method. These results can be explained by particular observations of the experiments in mice whose the two tumors were connected (Fig 24). In these cases, the presence of the primary tumor would not have influence on the other tumor growth.

Conclusion

To conclude, simulate with a reliable model allows to realize virtually difficult experiments. Indeed, we can observe the evolution of the tumor's volume over time without training the death of the subject caused by the tumor.
In our present, it enables firstly to confirm that the concomitant resistance and consequent post-surgery metastatic acceleration have important implications. Indeed, the effect of the local tumor growth on progression of metastasis has a significant increase in the growth of secondary tumor following the primary tumor's excision found in some clinical cases.
Secondly, the simulation lets us test the impact of the local tumor's volume at day of the amputation on the metastatic acceleration. The study reveals a non-monotony of the metastatic acceleration that has already been observed in [Gorelik et al., 1978].
We do not have enough available data about the concomitant resistance but we should continue to investigate on the post-surgery metastatic acceleration, because it might lead to a new path of cancer treatment if these pre-clinical results might occur in human patients. Indeed, control the patient tumor burden which has been experimentally demonstrated in the prevention of the metastatic acceleration with neo-adjuvant therapy, might be more beneficial than surgery therapeutic option in some instances.

6 Bibliographic Reports on Dynamics of Metastasis

Concomitant resistance and consequent post-surgery metastatic acceleration have important implications.
We can extend the study of the concomitant resistance based on a mathematical model describing the simple interaction between two tumors in the same organism, by the development of mathematical models for the systemic dynamics of metastases. Here, we have the representation of a population of metastasis in interaction.
[Benzekry et al., 2014a] completed the work of [Iwata et al., 2000] which describes a growing population of metastases, by integrating the systemic inhibition of angiogenesis.
Hence, we summarize the fundamental mathematical tools from these two articles on dynamics of metastasis.

6.1 A Dynamical Model for the Growth and Size Distribution of Multiple Metastatic Tumors, [Iwata et al., 2000]

A major problem in the treatment for cancer therapy is the possible presence of multiple metastasis in addition to a primary tumor in patients.
Indeed, tumors are able to disseminate multiple tumor cells to form distant metastatic tumors.
Actually, clinical imaging techniques have difficulties to detect small sizes of metastases.
Then, the goal of [Iwata et al., 2000] in his article was to develop a dynamical model for the colony size distribution of multiple metastatic tumors that he compared the prediction of the metastases' behavior against computed tomography (CT) images of a patient having hepatocellular carcinoma in the liver.

6.1.1 The Mathematical Model

The mathematical model that [Iwata et al., 2000] presented estimates the number of tumors even undetectable and predicts the future behavior of metastases.

Assumptions : The mechanism of dissemination can be explained as :

- a primary tumor is generated from a single cell at $t = 0$ and grows at rate $g(x)$ per unit time
- the first tumor emits metastatic single cells at rate $\beta(x)$
- each metastatic cell becomes a new tumor and also grows at rate $g(x)$ spreading new nuclei of metastasis at rate $\beta(x)$

Moreover, Iwata supposed that the colonies are far enough from each other to not merge. He further assumed in his model that tumors are not eliminated by treatment or natural death.

Model : Thus, the mathematical model which describes the dynamics of the colony size of distribution is the von Foerster equation defined by :

$$\begin{cases} \dfrac{\partial \rho(x,t)}{\partial t} + \dfrac{\partial g(x)\rho(x,t)}{\partial x} = 0 & (4) \\ \rho(x,0) = 0 & (5) \\ g(1)\rho(1,t) = \displaystyle\int_1^{\infty} \beta(x)\rho(x,t)dx + \beta(x_p(t)) & (6) \end{cases}$$

Where,

x **:** the cell number

$x_p(t)$: the number of cells in the primary tumor at time t

$\rho(x,t)$ **:** the colony size distribution of metastatic tumors at time t with x cell number

$\rho(x,t)dx$ **:** the number of metastatic tumors whose sizes is in $[x, x+dx]$ at time t

$g(x)$: the rate of growth per unit time represented by the Gompertz expression :

$$g(x) = axlog(\frac{b}{x})$$

where a is the growth rate constant and b is the tumor size at the saturated level.

$\beta(x)$: the rate of metastatic single cells emitted defined by :

$$\beta(x) = mx^{\alpha}$$

where m is the colonization coefficient and α the fractal dimension of blood vessels in contact with the tumor (equal to $\frac{2}{3}$ if the tumor vascularity is on the surface of the tumor, and 1 if the distribution of the blood vessels is homogeneously in the whole tumor).
Thus, the colonization rate $\beta(x)$ is proportional to the number of tumor cells in contact with the blood vessels which are able to spread metastatic cells via the blood.

The transport differential equation (4) results from the development of :

$$\rho(x,t)\Delta x = \rho(x + g(x)\Delta t, t + \Delta t) \times ((x + \Delta x) + g(x + \Delta x)\Delta t - x + g(x)\Delta t))$$

This traduces that the number of tumor cells at time t whose size belongs to $[x, x+\Delta x]$ is equal to the number of tumors cells at time $t+\Delta t$ whose size is in

$$[x + g(x)\Delta t, (x + \Delta x) + g(x + \Delta x)\Delta t]$$

Indeed, a tumor of size x at time t grows to a tumor of size $x + g(x)\Delta t$ at time $t + \Delta t$.

The first initial condition (5) interprets that at $t = 0$ there are not metastatic tumor. The second boundary condition (6) means that the number of new metastatic single cells created per unit time at time t is the total quantity of metastastic cells released by metastatic tumors present and the primary tumor.

Moreover, the theoretical cumulative distributions are defined by :

$$N(x,t) = \int_x^\infty \rho(x,t)dx$$

The cells number in the primary tumor $x_p(t)$ is the solution of

$$\begin{cases} \frac{dx_p}{dt} = & g(x_p) \\ x_p(0) = & 1 \end{cases}$$

where the solution is $x_p(t) = b^{1-e^{-at}}$

6.1.2 Results

To assess the model, [Iwata et al., 2000] confronted it with clinical data observed before the treatment from CT images of a patient with a hepatocellular carcinoma as a primary tumor, which presented multiple metastatic tumors in the liver.
The observed data were cumulative size distribution of metastases at 432, 559, 632 days after the first diagnosis as a primary tumor.

His results showed that the whole clinical data fitted well with the theoretical cumulative distributions curves.
He plotted the colony size distribution of metastatic tumors which was monotonically decreasing due to the criterion $m > a\alpha log(\frac{b}{b^\alpha - 1})$ with the parameters obtained.
Moreover, it had a good prediction of the primary tumor growth with the observed data.
We also note that the estimated parameter α is close to $\frac{2}{3}$ meaning the tumor vascularity is superficial which was confirmed by CT imaging.

To conclude, Iwata constructed a dynamical model for the growth and size distribution of multiple metastatic tumors.

It can be used to predict the future behavior of metastasis, to estimate the number of small tumors undetectable with clinical diagnostic techniques and the times of origin of metastases.

6.2 Global Dormancy of Metastases Due to Systemic Inhibition of Angiongenesis, [Benzekry et al., 2014a]

Studies, particularly autopsy studies, demonstrate that most individuals even the most healthy adults possess small tumor lesions that they do not necessarily train to the death.
Indeed, these lesions will not progress or have very slow tumor growth and stay stable, it is the tumor dormancy phenomenon.

The phenomenon of concomitant resistance offers an explanation for this dormancy in secondary tumors which is caused by the presence of the primary tumor.
One of these explanations proposes that the primary tumor releases angiogenesis inhibitors via the blood leading to the inhibition of vascular development at secondary sites and to prevent their growth limiting the nutrients.
Indeed, tumor cells liberate stimulatory growth factors, such as vascular endothelial growth factor (VEGF), and angiogenesis inhibitory factors, such as angiostatin, endostatin or thrombospondin-1 molecules.

Then, the goal is to complete the [Iwata et al., 2000] mathematical model which describes a growing population of metastases, by integrating the systemic inhibition of angiogenesis.

6.2.1 The Mathematical Model

The proposed model describes the dissemination of population of metastases, the growth of the primary tumor taking into account angiogenesis and interactions among the various tumor sites.

This mathematical model in 2D is defined by :

$$\begin{cases} \partial_t \rho + \nabla.(\rho G) = 0 & [0,T] \times \Omega \\ -G(V,K;V_p,p) \bullet \nu(V,K)\rho(t,V,K) = \mathcal{N}(V,K) \times & \\ \{\int_\Omega \beta(V)\rho(t,V,K)dVdK + \beta(V_p(t))\} & [0,T] \times \partial\Omega^+ \\ \rho(0,V,K) = \rho^0(V,K) & \Omega \end{cases}$$

Where,

V_p, V **:** respectively the volume of the primary tumor and the metastases

K_p, K : respectively the carrying capacity of the primary tumor and the metastases

$\rho(t, V, K)$: the density of metastases having volume V and carrying capacity K at time t

$G(V, K; V_p, \rho)$: the tumor growth rate vector G is composed of a Gompertz model for the tumor volume growth, and second term for the carrying capacity K :

$$G(V, K; V_p, p) = \begin{pmatrix} aVln(\frac{K}{V}) \\ Stim(V, K) - Inhib(V, K; V_p, \rho) \end{pmatrix}$$

with,

$$Stim(V, K) = bV$$

where b is the equivalent of the concentration of angiogenic stimulating factors.

It is considered that the inhibition is global and results from inhibitory factors released by primary and secondary tumors.

$$Inhib(V, K; V_p, \rho) = dV^{\frac{2}{3}}K + eIK$$

where $dV^{\frac{2}{3}}K$ represents the local inhibition and $I(t; V_p, \rho(t, V, K))$ is the concentration of the inhibitor from the population of tumors of density ρ at time t

$\beta(V)$: the emission rate of new metastatic cells which depends only on the volume is :

$$\beta(V, K) = \begin{cases} mV^{\alpha} & \text{if } V \geq V_m \\ 0 & \text{otherwise} \end{cases}$$

This term quantifies the number of newly created metastases. Here, it is assumed that the very small metastases under the volume V_m do not spread new metastatic cells because they do not have access to blood circulation.

$\mathcal{N}(V, K) = \delta_{(V,K)=(V_0,K_0)}$: the repartition of metastases at birth

$\Omega = (V_0, +\infty) \times (0, +\infty)$: the domain for the possible values of (V, K)

Here, the transport differential equation in 2D traduces the same phenomenon of conservation of mass as [Iwata et al., 2000].
The first boundary condition describes that the number of new metastatic cells created per unit time is equal to the total number of cells released by the entire population of tumors.
ν is the unit normal vector to the boundary of the domain Ω and allows to select the incoming flux i.e the new cells to the domain. Indeed, here it is chosen that the new

created metastatic cells are cells of size V_0 with a initial carrying capacity K_0.

The total number of metastases is :

$$N(t) = \int_\Omega \rho(t, V, K) dV dK$$

The total metastatic burden is defined by :

$$M(t) = \int_\Omega V \rho(t, V, K) dV dK$$

The mean size of the metastases is :

$$\frac{M(t)}{N(t)}$$

6.2.2 Results

The data used come from Huang's report(2002) which are number and mean size of metastases and primary tumor over the time from mouse breast tumors.
Nevertheless, it is difficult to find metastases which manifest a global dormancy. Then, the systemic inhibition of angiogenesis is neglected with $I = 0$. Indeed, I does not have any impact on the model simulations.
The values parameters are obtained from literature, heuristic deviation, or by fitting the model to these data.

The model revealed a relevant goodness-of-fit with the data from primary tumor growth and from number and mean size of metastases.

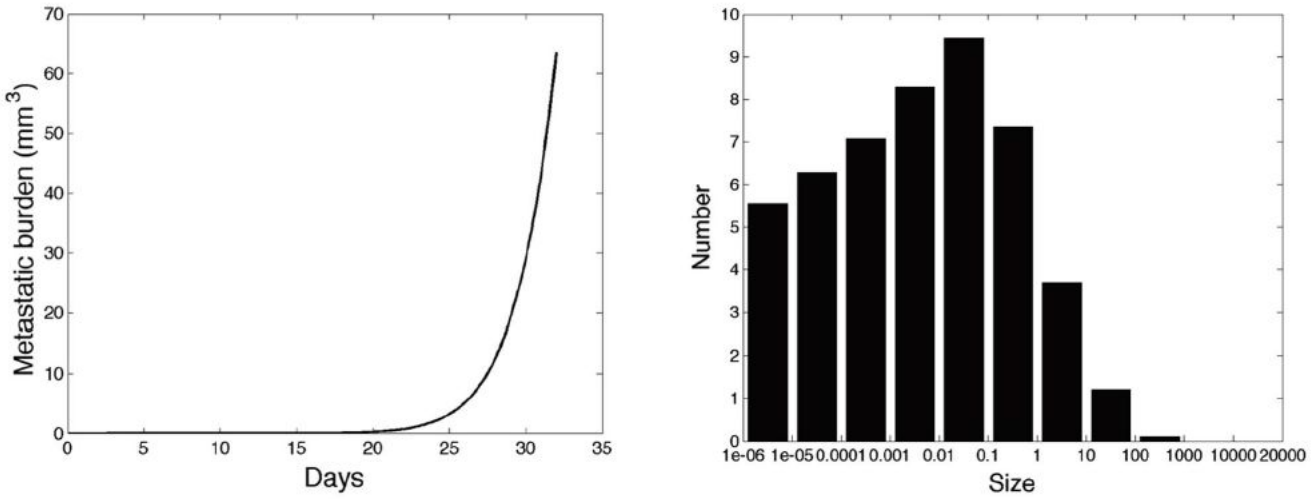

A. Metastatic burden

B. Colonies size distribution at the final time

Figure 3. *In silico* **simulation of the experiment from [56].** A. Time development of the metastatic burden. B. Colonies size distribution at the end time T = 32 days (log-scale on the x-axis).

Figure 31: [Benzekry et al., 2014a]

The parameter estimation allowed to simulate the experiment of Huang and returned (Fig. 31) the growth of the total metastatic burden and the colonies size distribution where it reveals a nontrivial size distribution at the end time of the experiment.
Then, the simulation also permitted to predict the cancer history starting from one initial tumor cells. It shows that the mouse would die from growth of its metastasis and not from the initial tumor.
The last result integrated the global dormancy represented by a high values of the parameter of inhibitor production rate p in large time simulation. It showed a possible convergence of the system to a steady state with the stabilization of the metastatic burden composed of small lesions.

To conclude, the model is able to describe data of primary tumor and metastasis development. It gives other information as the size distribution of metastases and their total number.
The model allows prediction of whole cancer history and lets the simulation of the systemic inhibition of angiogenesis which shows the stabilization of the cancer disease. Hence, the next step is to integrate in this global model the mathematical model of two tumors in interaction [Benzekry et al., 2016]. It could be beneficial and let a complete mathematical model of the concomitant resistance. It could also lead to personalized quantification of the impact of concomitant resistance in patients and to predict the post-surgical metastatic acceleration.

Conclusion

This internship met my expectations. Indeed, It was a first real work experience in my field of study. It also helped me to discover the research worker in the mathematical modeling.
I have strong knowledge in applied mathematics and I wanted to use these skills in the area of bio-medical, particularly I was proud to be involved in the cancer research and I hope that my investigation may help it. Working for a cause was very stimulating and motivating.

The internship was also professionally enriching because it gathered several competences : statistical tools, mathematical models based on ordinary differential equations, numerical simulations and knowledge of cancer biology.
I think that it was fascinating to study the limits of a mathematical model which describes the tumor growth in a specific instance («the concomitant resistance ») and to confront directly these mathematical tools against data obtained from real experiments. Additionally, I discovered many things about the cancer disease : the characteristics of tumor cells, the cancer cell formation, the treatments and the phenomenon of concomitant resistance. I globally obtained good results in my work, but I did not have the time to integrate the mathematical model of two tumors interaction in the global model of systemic dynamic metastatic.

This internship allowed me to be more determined on my professional project.

References

[Benzekry et al., 2014a] Benzekry, S., Gandolfi, A., and Hahnfeldt, P. (2014a). Global dormancy of metastases due to systemic inhibition of angiogenesis. PLoS ONE, 9(1):e84249.

[Benzekry et al., 2014b] Benzekry, S., Lamont, C., Beheshti, A., Tracz, A., Ebos, J. M., Hlatky, L., and Hahnfeldt, P. (2014b). Classical mathematical models for description and prediction of experimental tumor growth. PLoS Comput. Biol., 10(8):e1003800.

[Benzekry et al., 2016] Benzekry, S., Lamont, C., Hlatky, L., and Hahnfeldt, P. (2016). Dynamics of concomitant resistance: data, theories and mathematical modeling. In preparation.

[Chiarella et al., 2012] Chiarella, P., Bruzzo, J., Meiss, R. P., and Ruggiero, R. A. (2012). Concomitant tumor resistance. Cancer Lett., 324(2):133–141.

[Gorelik et al., 1978] Gorelik, E., Segal, S., and Feldman, M. (1978). Growth of a local tumor exerts a specific inhibitory effect on progression of lung metastases. Int. J. Cancer, 21(5):617–625.

[Gorelik et al., 1981] Gorelik, E., Segal, S., and Feldman, M. (1981). On the mechanism of tumor "concomitant immunity". Int. J. Cancer, 27(6):847–856.

[Iwata et al., 2000] Iwata, K., Kawasaki, K., and Shigesada, N. (2000). A dynamical model for the growth and size distribution of multiple metastatic tumors. J. Theor. Biol., 203(2):177–186.